Aus dem Institut für Physiologie und Pathophysiologie

Biochemical and mechanical investigation of cardiac titin isoforms

Inauguraldissertation zur Erlangung des

Doctor scientiarum humanarum (Dr. sc. hum.)

der
Medizinischen Fakultät Heidelberg
der
Ruprecht-Karls-Universität

vorgelegt von

Ciprian Neagoe

aus

Câmpina, Rumänien

2008

Dekan: Prof. Dr. med. Claus R. Bartram

Doktorvater: Prof. Dr. rer. nat. Wolfgang A. Linke

CONTENTS

LIST OF ABBREVIATIONS

Chemical reagents and solutions

AA-BA	solution of 30% acrylamide / bis- acrylamide, mixing ratio 37.5:1
APS	ammonium peroxydisulphate
ATP	adenosine 3' triphosphate
BDM	2,3-butanedione monoxime
BSA	bovine serum albumin
Ca^{2+}	calcium ion
$CaCl_2$	calcium chloride
CO_2	carbon dioxide
Cy3	cyanine derived fluorochrome
EGTA	ethylene glycol-bis(2-aminoethylether)-*N,N,N′,N′*-tetraacetic acid
FITC	fluorescein isothiocyanate
GA	glutaraldehyde
H_2O	water (distilled)
HCl	hydrochloric acid
KCl	potassium chloride
KH_2PO_4	potassium phosphate monobasic
K_2HPO_4	potassium phosphate dibasic
KOH	potassium hydroxide
MOPS	3-(N-Morpholino) propanesulfonic acid
$MgSO_4$	magnesium sulfate
NaCl	sodium chloride
$NaHCO_3$	sodium bicarbonate
Na_2HPO_4	sodium phosphate dibasic
NaOH	sodium hydroxide
NaN_3	sodium azide
NH_4Cl	ammonium chloride
PBS	phosphate buffered saline
PBS-Tx	phosphate buffered saline / 0.1% triton x-100
PFA	paraformaldehyde
PFA-Tx	4% paraformaldehyde / 0.1% triton X-100 / PBS solution
PI3K	phosphoinositol-3-kinase

SB	solubilization buffer
SDS	sodium dodecyl sulfate
TB	transfer buffer
TBS	tris buffered saline
TES	N-[Tris(hydroxymethyl)methyl]-2-aminoethanesulfonic acid
TEMED	N,N,N',N'-Tetramethylethylenediamine, 1,2-Bis(dimethylamino)-ethane
Tris	tris(hydroxymethyl)aminomethane
Tx	triton X-100

Measuring units

°C	degrees Celsius
h	hour
kcal	kilocalorie
kDa	kilodalton
M	mol per liter
mA	milliampere
MDa	megadalton
min	minute
ml	milliliter
mm	millimeter
mM	millimolar, (millimol per liter)
nm	nanometer
s	second
V	Volt
v/v	volumetric ratio
w/v	weight per volume ratio
µg	microgram
µl	microliter
µM	micromolar
µm	micrometer

Physical constants and measures in equations and graphs

A	persistence length
d	diameter
dpi	dots per inch

E	Young's module ~$7{,}7 \cdot 10^{11}$ mg/cm^2
f	force
FWHM	full width at half maximum
g	gravitational constant (9.81 m/s^2)
I	geometrical moment of inertia
i	intensity of the electric current
k_B	Boltzmann constant
L	contour length
LVEDP	left ventricular end diastolic pressure
MW	molecular weight
OV	optical volume (measured by TotalLab software)
pCa	negative decimal logarithm of molar Ca^{2+} concentration
pH	negative decimal logarithm of molar H^+ concentration
Q	electrical charge
SL	sarcomere length
z	chain extension
৬	displacement of the emitting fiber's tip
L	length of the optical fiber
V_0	maximum unloaded velocity of sarcomere shortening
ΔV	voltage, the electric potential difference between two measuring points

Other abbreviations

8I-7	a troponin I specific antibody
BD6	titin specific antibody BD6
CAD	coronary artery disease
CCD	charge-coupled device
COL1	a collagen I specific antibody, clone 1
cTnI	cardiac troponin I (also referred as c1, c2, d bands on Western blot)
DCM	dilated cardiomyopathy
e.g.	exempli gratia (lat.), for example
F	female
FH-7A	a collagen III specific antibody
FHC	familial hypertrophic cardiomyopathy
FN-3	fibronectin type-III-like

HH(s)	human heart(s)
i.e.	id est (lat.), that is
IFM	indirect flight muscles
Ig	immunoglobulin-like
IgG	immunoglobulin G
LAD	left anterior descending coronary artery
LDA	length-dependent activation
LV	left ventricle of the heart
M	male
MG1	MG1 antibody against titin
MHC	myosin heavy chain
MI	myocardial infarction
MyBP-C	myosin-binding protein-C
NYHA	New York Heart Association
N2-A	N2-A titin domain
N2B	titin isoform N2B or a specific segment of this isoform, when indicated
N2BA	titin isoform N2BA
N2BA-1	titin N2BA isoform of 3700 kDa
N2BA-2	titin N2BA isoform of 3500-3600 kDa
N2BA-3	titin N2BA isoform of 3200 kDa
N2BA-4	titin N2BA isoform of 3400 kDa
PEVK	PEVK domain of titin
RV	right ventricle of the heart
SS	Sommersemester (german)
SDS-PAGE	sodium dodecyl sulfate polyacrylamide gel electrophoresis
SEM	standard error of the mean
T1	full length, intact titin bands on gels
T2 or T3	the titin-degradation bands on gels
TnI	troponin I
uN2B	N2B-unique sequence
USA	United States of America
WLC	worm-like chain model of entropic polymer elasticity
WS	Wintersemester (german)

1. INTRODUCTION

1.1 Muscle contraction and three-filament model of the sarcomere

Already in the XIX century, striated muscle was known to produce active force during contraction. Also passive tension generation upon stretch was quantitatively described as a non-linear length-tension curve (Roy, 1881). The current concept for striated muscle contraction, the sliding filament theory, was proposed half a century ago (Huxley and Hanson, 1954; Huxley and Niedergerke, 1954). Accordingly, in the sarcomere, the structural unit of muscle, the interdigitating bundles of thick (myosin) and thin (actin) filaments slide past one another but do not change their actual length. The net result is a shortening or lengthening of the sarcomere. The muscle is hierarchically organized, in that serially linked sarcomeres form the myofibrils align parallel in the muscle fiber (myocyte). Many fibers build the fascicles (fiber bundles), which then form the whole muscle. Shortening of a whole muscle results from coordinated contraction of the individual fibers and the total shortening of a muscle fiber is close to the sum of the individual shortenings of the serially linked sarcomeres in the fiber.

Muscle function can be grossly distinguished in two states: a) the active state or contraction, in which the muscle produces work on the basis of ATP consumption, and b) the passive state, in which the muscle is not activated, but can still produce “passive work” when stretched from its resting length. These states can be readily described experimentally by three main parameters: force, length (change), and time, from which other parameters can be inferred: shortening velocity, work, and power output. In skeletal muscles, the active (developed) tension is typically much higher (>10 times) than the passive tension at physiological sarcomere lengths (SLs), whereas in cardiac muscle the relative contribution of passive to total (passive + developed) tension is quite substantial (Linke et al., 1994). Active tension has long known to be generated by the cyclic interaction between myosin heads and actin filaments. Passive tension also originates to a large part in the sarcomeres, namely in the elastic filament system. The existence of such a "third intrasarcomeric filament" holding actin and myosin filaments together was first proposed when thin and/or thick filaments were experimentally dissolved but the sarcomeres did not disintegrate (see Funatsu et al., 1990 and references therein). Maruyama et al. (1977 a, b) and Wang et al. (1979) proposed that the third filament is made of connectin (later named titin) molecules. Earlier concepts for passive

muscle elasticity, which had suggested that only extrasarcomeric, particular extracellular, elements (collagen) may be responsible for passive tension generation, were re-evaluated and the mechanical role of titin filaments soon became more generally accepted.

A step forward in the understanding of titin function was made when single titin molecules about one micrometer in size could be isolated from muscle and observed in the electron microscope (Figure 1) (Maruyama et al., 1984; Trinick et al., 1984; Wang et al., 1984; Nave et al., 1989). Subsequently it was shown that titin molecules reach across one half of a sarcomere, with the molecule's N-terminus anchored at the Z-disk and the C-terminus at the M-line. As the N-termini of titin from adjacent sarcomeres interact in the Z-disk and the C-termini of antiparallel titin molecules overlap in the M-line, a continuous filament system is formed in myofibrils. Titin may thus help center the thick filaments in the sarcomere.

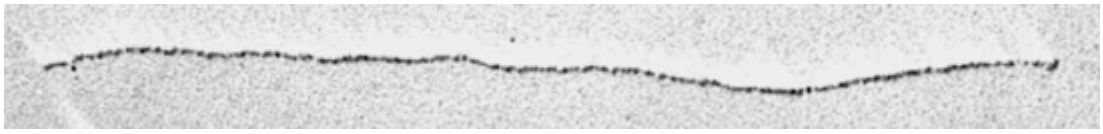

Figure 1. Electron micrograph of a single titin molecule purified from rabbit back muscle. The molecule is straightened by denaturant agents to ~1.3 μm length, which is close to the predicted length considering the primary structure (from Tskhovrebova et al., 2002).

1.2 Molecular structure of titin - one gene, multiple isoforms

Sequencing of the A-band part of human titin showed that this section of the molecule is composed of ~42-nm long super-repeats of immunoglobulin-like (Ig-) and fibronectin type-III-like (FN-3-)domains (Figure 2), which regularly bind myosin tails and myosin-binding protein-C (MyBP-C) along the thick filament (Labeit et al., 1990, Fürst et al., 1989). Ig and FN3 sequence motifs result in ~4 nm diameter globular polypeptide modules (Trinick et al., 1984; Whiting et al., 1989) with tertiary structure of 7 or 8 antiparallel beta sheets (Leahy et al., 1992; Pfuhl and Pastore, 1995; Politou et al., 1995). The structure of A-band titin is highly conserved among mammalian muscles. The A-band titin region binds not only myosin and MyBP-C, but also associates near the M-line region with a number of other ligands (Figure 2), such as the M-line proteins, myomesin and M-protein (Obermann et al. 1995; 1996; 1997; van der Ven and Fürst, 1997). There is a kinase domain near the M-line titin (Figure 2) which is involved in protein-protein-interactions and myocyte signalling (reviewed by Trinick and Tskhovrebova, 1999; Gregorio et al, 1999; Clark et al. 2002).

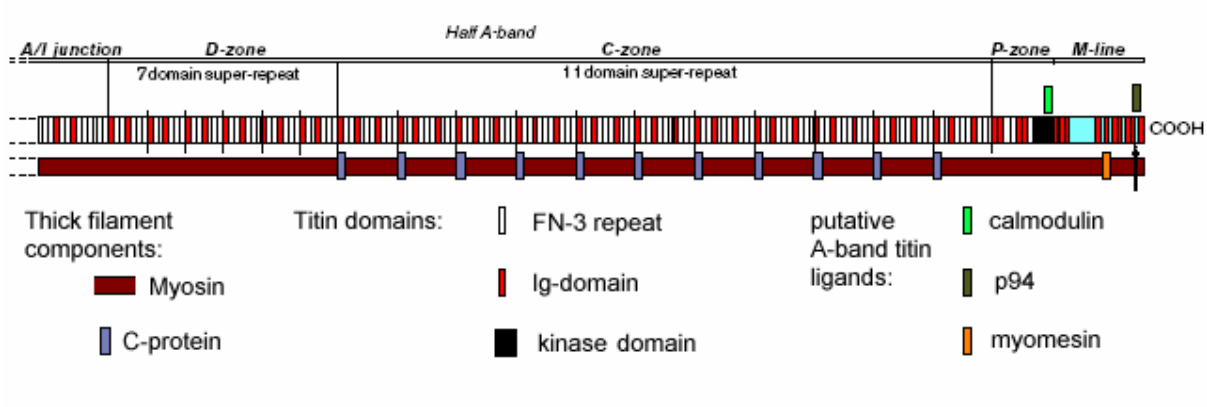

Figure 2. A-band titin structure. Super repeats composed of Ig and FN-3 domains have regular sites binding myosin tail and thick filament associated C-protein (MyBPC). Various titin ligands were identified by in vitro studies with antibodies, recombinant titin fragments and yeast two-hybrid systems (modified from Gregorio et al., 1999).

A-band titin possibly is a template upon which other proteins are arranged during sarcomerogenesis (Whiting et al., 1989). For instance, A-band titin may determine the precise assembly of thick filaments, because the periodicity of its super-repeat pattern matches that of the myosin heads (reviewed by Trinick and Tskhovrebova, 1999).

Publication of the full-length human titin sequence (Labeit and Kolmerer, 1995) was final proof for the proposal that a single polypeptide chain the size of 3000 kDa or more (up to >38,000 residues) exists in muscle cells. Sequencing demonstrated the presence of 3000-4000-kDa proteins generated by differential splicing from the copy of a single titin gene. Titin has a modular structure consisting of up to 166 Ig-domains, 133 FN3-repeats, and many unique sequences. Whereas the A-band titin is constitutively expressed, differential splicing of I-band titin gives rise to titin isoforms differing greatly in size in different muscles (Figure 3). Analysis of the titin genomic structure and further sequencing (Freiburg et al., 2000; Bang et al., 2001) established the alternative splicing pathways for human and rabbit titin isoforms (Figure 3B). I-band titin has no FN3 domains. Instead it has Ig-domains arranged in tandem. Most tandem-Ig modules are grouped in two segments, 'proximal' and 'distal' to the Z-disk, flanking a region that has many unique sequences. The Ig-domains in I-band titin are not identical; they can be grouped in subfamilies on the basis of sequence homology. The Ig-domains from different subfamilies are compiled in long-range patterns or 'super-repeats' consisting of 6 or 10 domains (Witt et al., 1998).

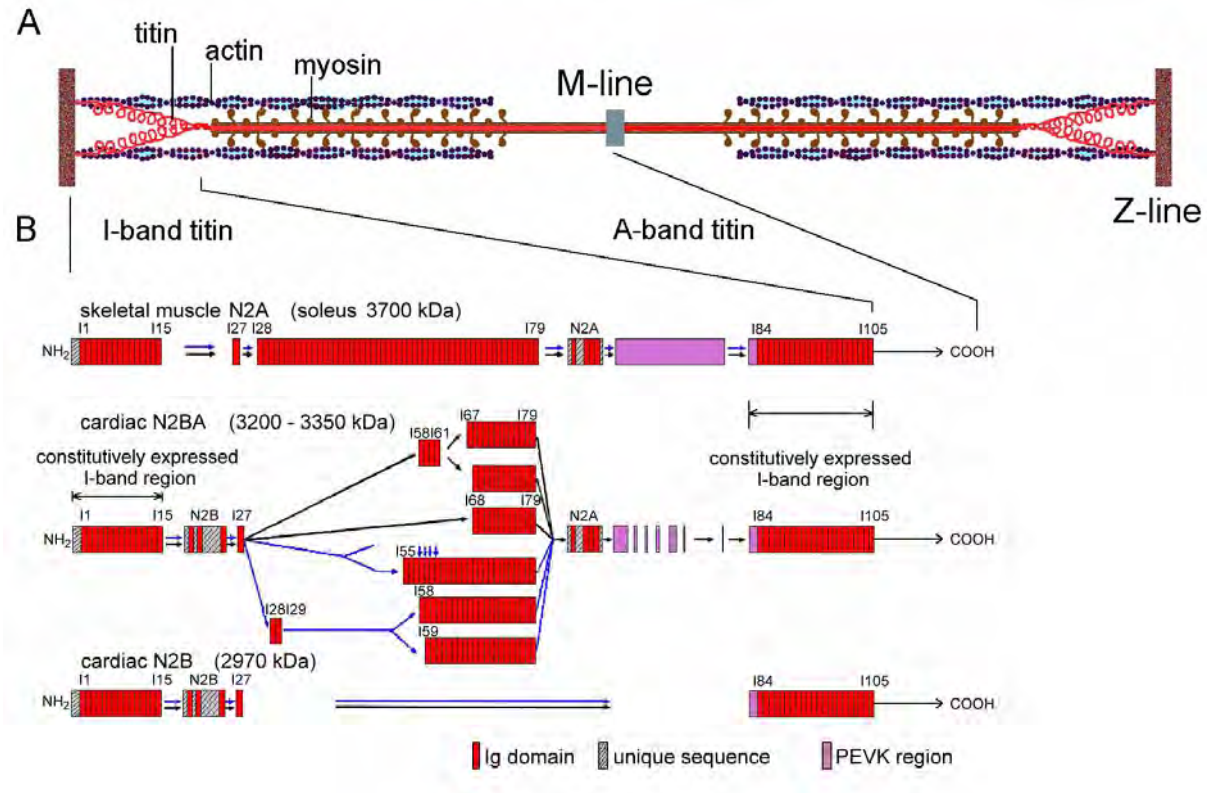

Figure 3. Layout of titin in the sarcomere and I-band titin structure. A. Schematic of the sarcomere as a three-filament structure: thin (actin), thick (myosin) and elastic (titin) filaments. B. Alternative splicing pathways for I-band titin in human (black arrows) and rabbit (blue arrows) soleus and cardiac muscles (modified from Freiburg et al., 2000).

The longest unique sequence is the PEVK-domain (rich in proline, glutamate, valine and lysine residues). The PEVK-domain is expressed in the cardiac N2B-isoform as a 190-residue chain, whereas in other isoforms (skeletal N2A, embryonic cardiac N2BA) it can reach up to 2200 residues (e.g., in human soleus muscle) (Labeit and Kolmerer, 1995). There are additional unique sequences in I-band titin, e.g., in the so-called N2A-domain (Figure 3). Further, the N2B-domain domain is expressed only in cardiac titin isoforms; it contains a so-called "N2B-unique sequence" (uN2B) which has 572 amino-acid residues (Figure 3).

Titin isoforms differ in the number of Ig-modules they contain and the length of the PEVK-region. Also the presence/absence of the N2B or N2A domain distinguishes the titin isoforms. The largest titin isoform sequenced so far is a 3.7 MDa N2A-titin from human soleus muscle (Freiburg et al., 2000; Trombitas et al., 2001). In comparison, rabbit psoas-muscle titin has 3.3-3.4 MDa, whereas human cardiac sarcomeres co-express two isoform types, N2BA-titins (3200-3700 kDa) and N2B-titin (3000 kDa). A ~700-kDa titin isoform, Novex-3, was discovered by Bang et al. (2001). This isoform seems to be expressed in low

abundance in striated muscles, but its function is still unclear.

I-band titin segment is elastic and extends during skeletal muscle stretching (Fürst et al., 1988; Itoh et al., 1988; Whiting et al., 1989; Gautel and Goulding, 1996, Linke et al., 1996, Linke et al. 1998b). Similarly, I-band titin is a molecular spring in cardiac sarcomeres (Linke et al., 1996, Granzier et al., 1997, Linke et al 1998b; Linke 2000). Titin elasticity in cardiac myocytes was shown to depend on titin-isoform expression (Linke et al., 1996; Cazorla et al., 2000; Freiburg et al., 2000). Interestingly, titin may have a role in the stretch-dependent enhancement of active myocardial force production (length-dependent activation), the basis for the Frank-Starling mechanism (Fukuda et al., 2001; Cazorla et al., 2001).

The titin springs are anchored in the Z-disk via α-actinin (Figure 4). The amino terminus of titin in the Z-disk contains seven titin Z-repeats involved in multiple interactions with α-actinin (Ohtsuka et al., 1997; Young et al., 1998). The extreme NH_2-terminus binds Telethonin (T-cap), which acts as a capping protein for titin (reviewed by Trinick & Tskhovrebova 1999, Clark et al. 2002).

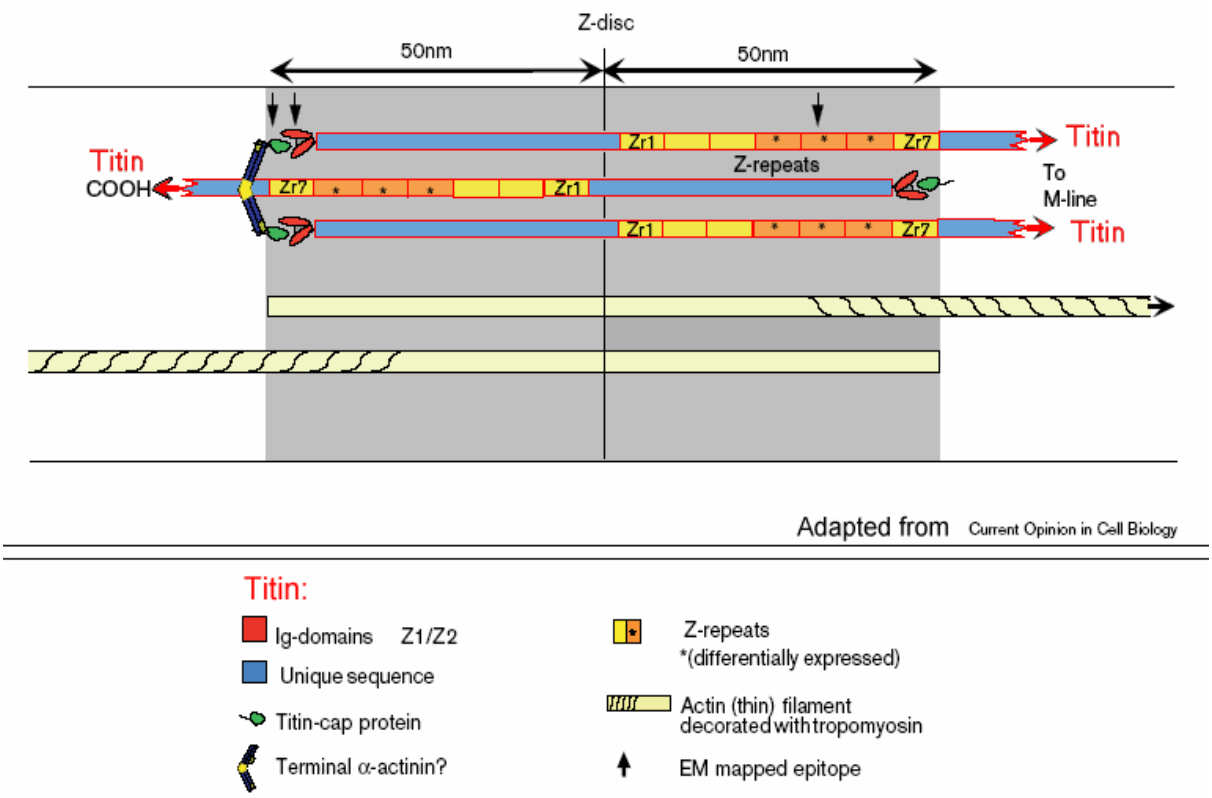

Figure 4. Titin anchorage in the Z-disk. A ~80 kDa region of titin is composed of seven repeats of 45 amino-acid residues (Z-repeats). Z-disk titin interacts with telethonin (T-cap) and α-actinin, proteins that anchor titin in the Z-disk (adapted from Gregorio et al., 1999).

1.3 Sources of I-band titin elasticity

By using immunolabelling techniques with anti-titin antibodies, the extensibility of I-band segments was studied in skeletal and cardiac sarcomeres (Linke et al., 1996; Helmes et al., 1996; Linke et al., 1998 a, b). Force measurements were performed at different structural levels, on single cells (Helmes et al., 1996), single myofibrils (Linke et al., 1996; 1998 a, b) and single titin molecules or recombinant titin fragments (Rief et al., 1997; Kellermayer et al., 1997; Tskhovrebova et al., 1997). The elasticity of the non-activated sarcomere could be described as the sum of the extensible properties of the titin constituting modules (Li et al., 2002). These studies led to the following titin extension model (Figure 5): at low stretch the linker regions between proximal and distal Ig-domains straighten out. With further stretch, the PEVK-domain and then the uN2B extend (Linke et al., 1999; Helmes et al., 1999).

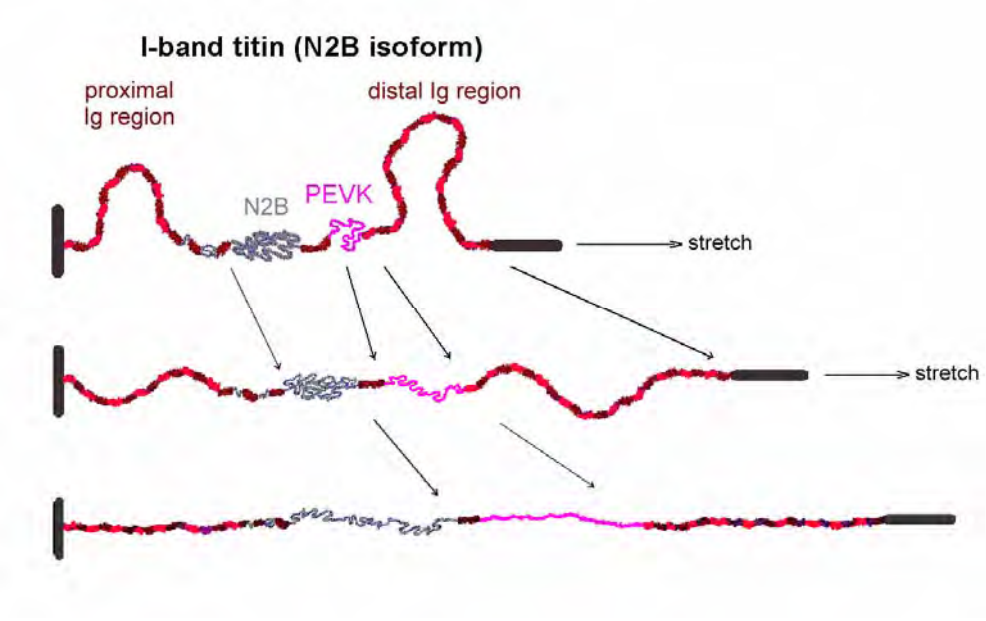

Figure 5. Sequential extensibility of I-band segments in cardiac titin. At low force, the main contribution to the extension of the titin molecule comes from straightening the inter-Ig-domain linkers. Further extension is provided by the PEVK and the uN2B domains (modified from Linke et al., 1999).

Another source of titin extensibility is the unfolding of I-band Ig-domains, which can suddenly add substantial length (~30 nm per unfolded domain) to a titin molecule. The rate of unfolding depends on the applied force and the rate of stretch (Evans and Ritchie, 1999; Li et

al., 2002). Unfolding explains much of the stress relaxation and may constitute a mechanism to reset the force to a lower level after the muscle had been extended (Minajeva et al., 2001). It may also work as a safety mechanism to prevent overloading the muscle (Tskhovrebova and Trinick, 2000; Minajeva et al., 2001). The physiological relevance of Ig-domain unfolding is still controversial. Ig-unfolding events occur with high probability only at forces reached towards the upper end of the physiological sarcomere-length range. However, even lower rates of Ig-unfolding at modest stretch forces could impact the passive tension in skeletal myofibrils over much of the physiological length range (Minajeva et al., 2001). At zero external force, the free energy of unfolding is between 2 and 10 kcal mol^{-1}, unfolding rate constants are in the range 10^{-2} to 10^{-6} s^{-1}, and folding rates are between 10^{-2} and 10^{2} s^{-1} (Scott et al., 2002; Head et al., 2001). Titin Ig-domains adopt a beta sheet fold. Between antiparallel strands hydrogen bonds are established that can reversibly break under external force, thus causing domain unfolding (Carrion-Vazquez et al., 1999). The consequence of domain unfolding is that chain tension drops as this event extends considerably the length of the stretched segment. Following a stretch, unfolded Ig-domains could refold (Trombitas et al. 2003). The ratio between unfolded and refolded domains increases with SL and force (Linke and Fernandez, 2003). In turn, when titin molecules are released to zero external force, refolding occurs more frequently than unfolding and an equilibrium conformation is established.

In contrast to the Ig-domains, the PEVK-region has no apparent secondary structure. The amino-acid residues of this domain are highly charged at physiological pH. The PEVK-derived titin contribution to myofibrillar stiffness is ionic-strength dependent and PEVK elasticity has been proposed to be based on both entropic mechanisms and electrostatic interactions (Linke et al., 1998 a). The PEVK region is considered to adopt random coil conformation; however, the repetitive motifs in the sequence (Greaser, 2001) suggest some degree of internal organization which possibly has structural and functional consequences.

1.4 Theoretical models of titin elasticity

Mathematical models of titin elasticity were adapted from elasticity theory developed for polymers (Kellermayer et al., 1997; Rief et al., 1997; Tskovrebova et al., 1997). In the relaxed state, a polymer adopts a collapsed structure characterized by maximum segmental entropy. Under an external force the entropy decreases and an opposing force is generated to restore the initial state. The worm-like chain (WLC) model (Marko and Siggia, 1995) of entropic elasticity was shown to adequately describe the experimental force-extension curves

obtained from titin experiments (Granzier et al., 1997; Linke et al., 1998 a, b). The model considers polymers as continuous strings of a given contour length (L) and persistence length (A), the latter reflecting the polymer's bending rigidity (stiffness). In the WLC model, the external force (f) is related to chain extension (z) through:

$$f = \frac{k_B T}{A}\left[\frac{1}{4(1- z/L)^2} - \frac{1}{4} + \frac{z}{L}\right], \qquad (1)$$

where T is absolute temperature and k_B is the Boltzmann constant. The smaller the persistence length, the higher is the external force needed to extend the polymer. According to this model, titin behaves primarily as an entropic spring capable of fully restoring the initial length immediately, once the external force is removed.

The titin Ig-domain regions showed a force-extension relation consistent with pure WLC behavior (Linke et al., 1998 b) (see Figure 6, inset). In contrast, the PEVK-domain was shown to behave like a pure entropic spring at shorter SLs but deviate from this behavior at longer lengths (Linke et al., 1998 a). An enthalpy term added to the WLC equation corrected the divergence between model and experiment (Figure 6), explainable by the contribution of electrostatic interactions to PEVK elasticity. Another experimental indication for an enthalpy term was the force hysteresis observed in stretch-release experiments of single myofibrils or titin molecules (Minajeva et al., 2001; Kellermayer et al., 2001). Titin thus appears to be more a viscoelastic than a purely elastic spring.

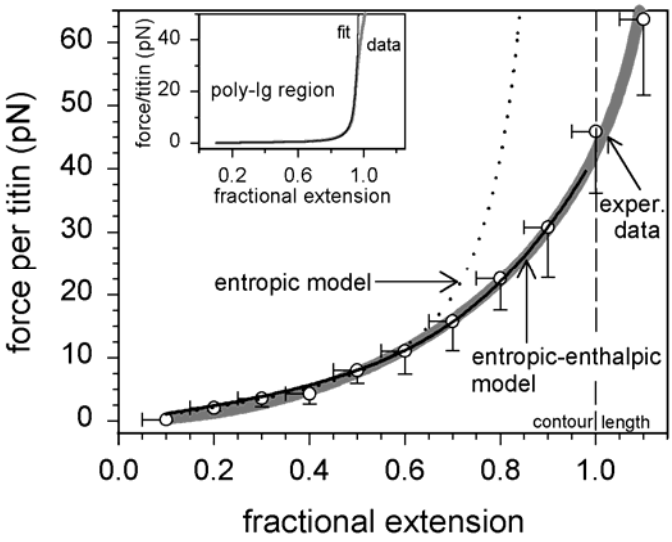

Figure 6. Force–extension relation of titin segments in rat psoas muscle. The dotted line is a fit of PEVK-domain elasticity according to the WLC model, the continuous black line is a simulation using the WLC model with an enthalpic contribution. Inset: Pure WLC fit applied to the proximal poly-Ig region (from Linke et al., 1998 a).

A recent report showed using two-bead optical tweezers that two entropic springs act in series in the I-band of skeletal titin molecules, one assigned to tandem-Ig domains, the other to the PEVK-region. The study suggested that an enthalpic component derives in part from unfolding of structured elements (tandem-Ig domains) and that also some structures in the PEVK-domain contribute to enthalpic elasticity (Leake et al., 2004).

In cardiac titin, an additional extensible element is the uN2B and the cardiac titin isoforms were therefore proposed to be three-element molecular springs (Linke et al., 1999). Accordingly, a three-element in-series WLC model readily described the (visco)elasticity of human heart titin (Li et al., 2002; Opitz et al., 2004; Makarenko et al., 2004). A source of the viscous component is the interaction of titin with actin filaments in the sarcomeres (Kulke et al., 2001 b; Minajeva et al., 2002; Linke et al., 2002 a), which cause damped elastic recoil of the titin springs from a stretched conformation (Opitz et al., 2003).

1.5 Titin molecules are differentially expressed in various muscle types

Nature has adopted differential splicing of titin isoforms as a way to tune sarcomeric passive stiffness. Variation of the total length of the titin molecule is achieved by including a variable number of Ig-modules in the titin I-band chain or by altering the number of PEVK residues. A longer titin generates less entropic force than a shorter titin at a given SL.

Mammalian cardiac muscles express not only one major titin isoform (as for example soleus or longissimus dorsi muscles do); instead two titin isoforms (N2B and N2BA) with different elastic properties are expressed in the myocardium. Linke et al. (1996) demonstrated that co-expression of both isoforms occurs at the myofibrillar level. Trombitas et al. (2001) showed both isoforms to be co-expressed in the same half-sarcomere. Hence, titin stiffness can also be tuned by variation of the titin-isoform composition, while the total number of titins in the sarcomere remains fixed at most likely six titin strands per half thick filament (Liversage et al., 2001).

Recently our group compared the titin N2BA:N2B expression ratios between normal and failing myocardium and showed that this ratio indeed varies, which then affects the sarcomeric compliance (Neagoe et al., 2002). This work, as well as the titin-isoform expression in various species, in various muscles of a given animal, and a map of titin isoform expression in heart (Neagoe et al., 2003), will be a focus of this thesis.

1.6 Titin and collagen are sources of passive tension in cardiac muscle

Cardiac muscle is a remarkable machine as it functions over a lifetime without pausing. Proteins are renewed (turned over) and the effects of excessive stress are compensated while the muscle works. However, injuries can cause irreversible damage to the heart's structure and function and cause cardiomyopathies and eventually, heart failure.

The work produced in a heart cycle (Figure 7) originates in actin-myosin filament sliding which changes the SL. The third filament of the sarcomere, the titin, bears the mechanical (passive) forces exerted during diastolic filling of the heart chamber.

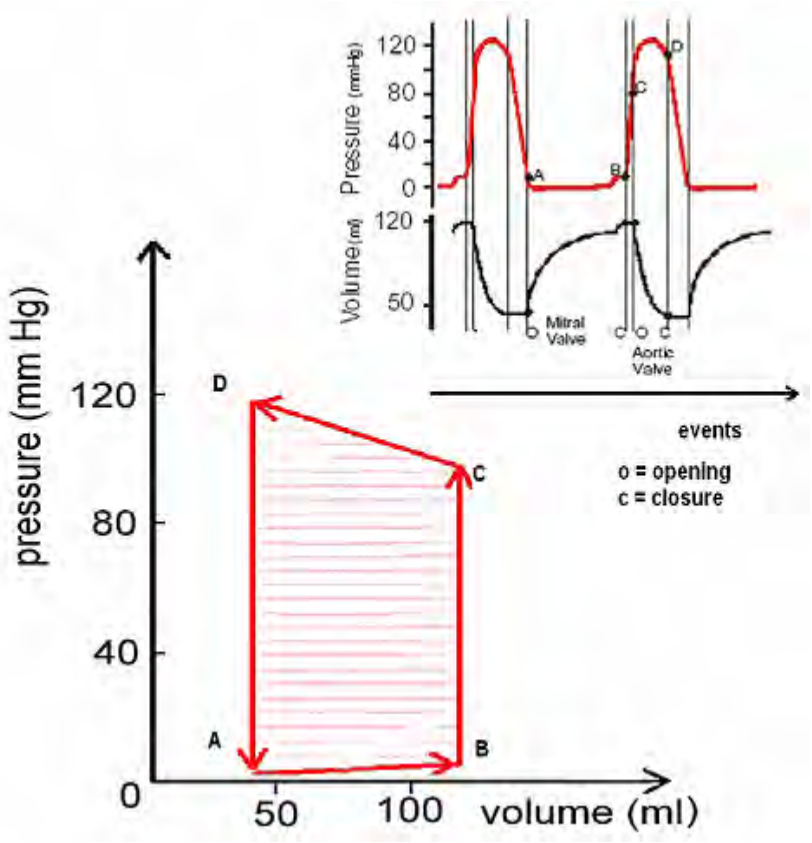

Figure 7. The heart cycle. Pressure-volume diagram and opening - closure events occurring with the mitral and the aortic valves during one cycle of the heart. Titin is a major contributor to the A-B segment, which represents the diastolic filling.

Ventricular wall resilience results from several contributions. Titin is, together with collagen/connective tissue, a main determinant of the end-diastolic pressure (Linke et al., 1994; Granzier and Irving, 1995). At SLs lower than 2.2 μm the tension in a cardiac muscle strip is generated by titin (Linke et al., 1994). Extracellular collagen fibers are rigid structures

and probably slack when the sarcomeres are shorter than 2.2 µm. They are likely to limit further extensibility of the muscle once they become stretched at >2.2 µm SL (Figure 8).

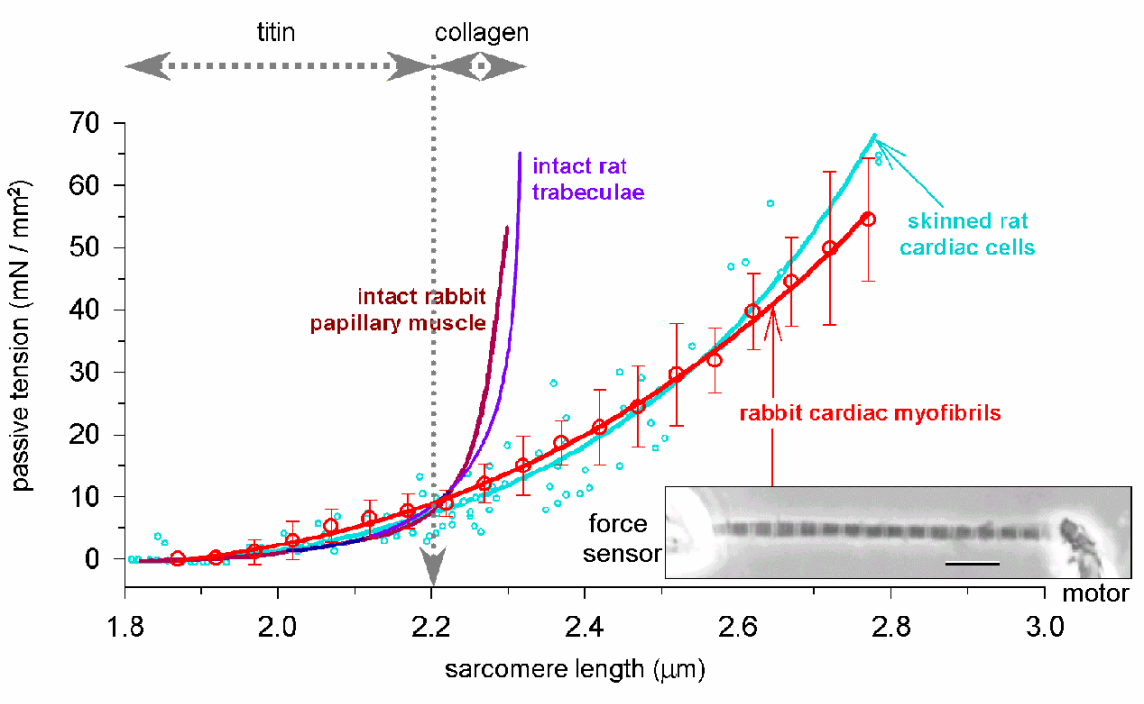

Figure 8. Sources of passive tension in cardiac muscle. Comparison of the passive tension-extension curves obtained from muscle strips (containing extracellular structures) and myofibrils (where titin is the main determinant of stiffness). At SLs above 2.2 µm, collagen determines a steep rise in the passive tension response of the muscle. Inset: phase image of myofibril specimen; scale bar, 5 µm (from Linke et al., 1994, 2000, 2002 b).

1.7 Heart failure can be associated with defects in cytoskeletal proteins

Heart failure is defined as a state of the myocardium in which cardiac function is impaired. Work output is not sufficient to adequately supply metabolic nutrients and oxygen to the body. Ischemic heart disease, valve defects, hypertension, or cardiomyopathies, all may evolve to heart failure. Progression from cardiac abnormalities to heart failure involves changes in the expression of many proteins. In the early phase of compensated myocardial hypertrophy the ventricular mass is increased with the tendency to normalize the wall stress. From this point on, the influence of yet-undefined stimuli may lead to decompensated cardiomyopathy characterized by cellular atrophy and interstitial fibrosis.

Hereditary defects in genes coding for sarcomeric proteins or in genes coding for

cytoskeletal proteins have been associated with cardiomyopathies. Familial hypertrophic cardiomyopathy (FHC) appears to be primarily a disease of the sarcomere, as most of the disease-causing mutations are found in genes encoding sarcomeric proteins, i.e., beta-myosin heavy chain, MyBP-C, alpha-tropomyosin, troponin I, troponin T, actin, or titin. In contrast, multiple lines of evidence support the concept that heart failure resulting from inherited forms of dilated cardiomyopathy (DCM) may occur primarily due to defects in the expression of cytoskeletal proteins (for review see Bowles et al., 2000), e.g., in genes encoding dystrophin or actin. In another example, mutations in the 53-kDa protein desmin, which contributes to cytoskeletal organization in muscle by connecting sarcomeres through their Z-disks and stabilizing the muscle structure, cause DCM by weakening these connections (Li et al., 1999). As for titin, cardiomyopathy-causing mutations have been described in the Z-disk region, the Z-I transitional zone, the N2B-domain, and the A-band region (Gerull et al., 2002). Mutations in the titin gene were found in human and zebrafish hearts.

Cardiomyopathies are not only caused by gene mutations. Environmental factors can be another stressor leading to heart disease. For example, ischemia caused a shift in myosin heavy chain expression from the fast type to the slow type, presumably diminishing the energy utilization rate during a heart cycle (Schaub et al., 1997, and references therein). Myocardial isoform switching could be a general phenomenon associated with many types of heart disease. Titin was earlier shown to be disrupted in idiopathic DCM, which was interpreted as proteolytic damage to the titin filaments and consequently deficiencies in force transmission and mechanical stress handling (Hein et al. 1994; Morano et al. 1994). These conclusions were drawn based on the results of immunofluorescence microscopy studies on tissue sections using anti-titin antibodies. In my thesis, a goal was to determine whether titin-isoform expression is altered in two types of human cardiac disease, ischemic coronary artery disease (Neagoe et al., 2002) and non-ischemic DCM (Makarenko et al., 2004). The results will be presented and commented below.

1.8 Cardiac titin and active muscle contraction

Systole is powered by active force production in the sarcomeres, but what about the elastic energy stored during diastole? Is it lost as heat or is it converted into work to support muscle contraction? Experiments showed that titin-derived elastic forces in stretched skeletal myofibrils cause very fast passive shortening under zero external loads (Minajeva et al., 2002). Under active conditions, the passive elastic recoil of titin could still support active

contraction in the very early phases of shortening. Similar conclusions were drawn from experiments on human cardiac myofibrils. It was proposed that the passive elastic energy stored in the titin springs helps the early phase of active shortening, before titin elastic recoil is quickly damped by viscous resistive forces (Opitz et al., 2003).

Increased viscosity inside cardiomyocytes has long been known to alter cardiac function, as viscosity interferes with filament sliding and can limit the shortening velocity of cardiac sarcomeres. A viscous force was initially experimentally observed in cat papillary muscle at moderate stretch velocities (Noble, 1977). This viscous force was later proposed to originate in the microtubule network and/or weak cross-bridge interactions. Recently it was shown that a viscous force arises from titin-actin interactions (Kulke et al., 2001 a; Yamasaki et al., 2001; Linke et al., 2002 a) and more precisely, from interactions between actin and titin's PEVK-domain. This drag force was temperature and calcium dependent (Kulke et al., 2001 a). The length of the PEVK region is subject to substantial variations owing to alternative splicing of titin isoforms. Thus, changes in titin-isoform expression could also modify the viscous properties of the sarcomere, e.g., in heart disease.

An essential mechanical property of the heart is the preload-dependent force enhancement in the active contraction phase, best known as the Frank-Starling law of the heart. The molecular basis for this phenomenon is still unknown, but involves an increase in calcium sensitivity of active force production upon stretch of the muscle. Interestingly, when titin was selectively degraded by very low concentrations of trypsin, passive tension dropped and cardiac fibers lost their ability to become sensitized to Ca^{2+} by stretch (Cazorla et al., 2001; Fukuda et al., 2001). Titin could thus play a role in length-dependent activation (LDA). A possibility is that titin affects the lateral filament spacing between actin and myosin filaments (Figure 9), which has been suggested to be important for LDA (Moss and Fitzsimons, 2002).

Another proposal to explain LDA in cardiac fibers is based on the fact that titin strands and thick filaments are bound together in the A-band region (Muhle-Goll et al., 2001). The strain imposed by stretch of the sarcomere may be transmitted via I-band titin to the A-band section of titin, thereby affecting myosin head periodicity and/or motor properties of cross-bridges. However, additional investigations are required to directly link titin and the Frank-Starling mechanism.

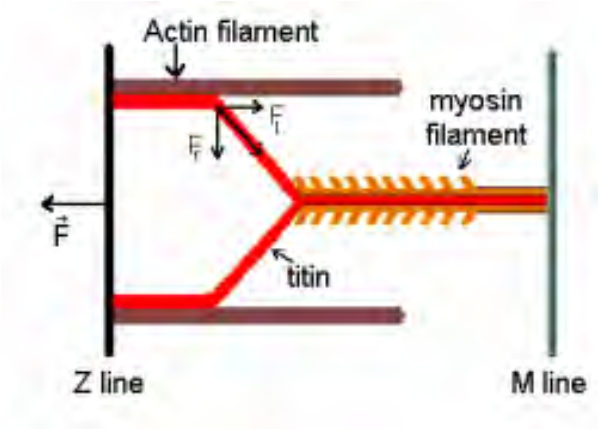

Figure 9. Myofilament arrangement and illustration of how titin could control lattice spacing (from Moss and Fitzsimons, 2002). A radial component of titin-based tension exerts compression on the space between actin and myosin filaments (lattice spacing). The probability of crossbridge interaction may increase at long SLs, since actin filaments and crossbridges are closer to each other.

The Frank-Starling mechanism is sometimes compared to the stretch activation response seen in insect indirect flight muscles (IFM), although these two phenomena may be unrelated (Vemuri et al., 1999). Interestingly, there are two homologues of titin in IFM, kettin and projectin (Kulke et al., 2001 a). Recently it was suggested that expression of different-length kettin-isoforms modulates the passive tension in Drosophila IFM (Leake et al., 2003), perhaps influencing stretch activation. Similarly, altered titin-isoform expression (e.g., in failing hearts) could affect the ability of the heart to sense the diastolic preload.

In conclusion, investigation of cardiac titin expression is relevant for understanding at the molecular level the mechanical properties of cardiac muscle, particularly in diastole but also in systole. This thesis was aimed at determining the role of titin in normal and diseased hearts. A focus was the titin-isoform diversity in different muscle types and the pathological changes in cardiac titin expression and function in human hearts. Most results shown and discussed here have been published in original peer-reviewed research articles.

2. MATERIALS AND METHODS

2.1 Tissue

2.1.1 Human heart tissue

Studies on human heart (HH) tissue were approved by the Subcommittee on Human Research at Massachusetts General Hospital. Left ventricular samples (anterolateral midwall) from 29 HHs were collected in accordance with the approved guidelines. Samples were classified in 5 groups:

1) CAD transplant – hearts from patients with coronary artery disease (CAD) characterized by a history of multiple infarcts; New York Heart Association (NYHA) class III-IV;
2) CAD donor – hearts that show significant signs of CAD but no antecedents of diagnosed heart disease;
3) non-ischemic transplant - hearts transplanted for reasons other than CAD;
4) DCM transplant – hearts diagnosed with dilated cardiomyopathy (DCM) and explanted in transplantation surgery; NYHA class III-IV;
5) normal donors – non-failing hearts obtained from brain-dead human donors, for which normal LV function had been confirmed by echocardiographic evidence.

From these hearts, non-necrotic regions were studied as detected by gross examination of the ventricles cut in transverse sections. Transplant HH were transported for ~1 h and donor HH for 1 to 5 h in cardioplegia, then deep frozen at –80°C.

2.1.2 Tissue samples and preparation of myofibrils

Laboratory animals were sacrificed according to institutional guidelines. In most cases the animals were obtained from the University of Heidelberg' s animal house. Occasionally tissue was obtained from local slaughterhouses in Heidelberg. Rat samples with a ligature of the left anterior descending coronary artery (LAD) were from animals used in a previous study by Dr. Pieter de Tombe, University of Illinois, USA; animals were purchased from Charles River Laboratories. Frozen heart tissue was shipped to Heidelberg on dry ice.

The following muscles were of particular interest: heart, soleus, and psoas major. Skeletal muscles were rinsed and hearts perfused with ~20 ml of extracellular solution "Rigor 1" (see 2.4 Solutions). Hearts were dissected, the LV separated from the RV, and tissue

quickly frozen in liquid nitrogen. In some cases trabecular fibers (3-5 mm long and 200-400 μm thick) were cut from freshly excised LV tissue. Muscle strips (~1 mm thick and 1-2 cm long) were cut along the fiber orientation, the ends tied to a glass rod, and then skinned in 0.5% Triton X-100 / Rigor 2 buffer supplemented with leupeptin (40 μg/ml) for 4 to 12 h (4°C, under continuous shaking). In case of human hearts the muscle fibers were dissected from frozen tissue. The Triton X-100 was washed out with Rigor 2 buffer and the fibers were incubated for 1h in ice-cold Rigor 2 buffer + leupeptin. When not prepared for fiber mechanical measurements, the strips were used to obtain myofibrils. Fibers were minced and homogenized with an Ultra Turrax homogenizer (IKA-Werke, Hannover, Germany). At the end of the procedure one could find structurally intact, isolated myofibrils in the myofibril suspension.

2.2 Antibodies

2.2.1 Primary antibodies

The following anti-titin antibodies were used: MG1 to N2BA-titin (N2A domain), N2B to N2B domain and BD6 to all titin isoforms (Whiting et al., 1989; Linke et al., 1999; Gautel et al., 1996). For epitope localization, see Figure 10. Cardiac troponin I, cTnI, was detected with antibody 8I-7 (Spectral Diagnostics, Canada) (McDonough et al., 1999; Feng et al., 2001). To identify collagen I and collagen III, COL1 or FH-7A were used (Sigma-Aldrich). Desmin antibodies were from Progen Biotechnik (Germany).

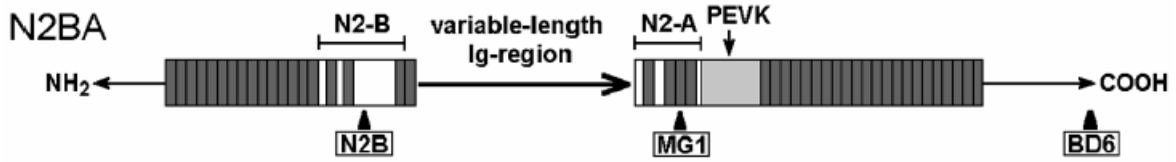

Figure 10. Sequence assigned titin antibodies used for this study: localization of the respective epitopes on N2BA-titin (from Neagoe et al., 2002).

2.2.2 Secondary antibodies

All secondary antibodies were purchased from Sigma-Aldrich. For fluorescence microscopy, Cy3 or FITC dyes conjugated with anti-rabbit or anti-mouse IgG antibodies

were used. Dilutions were used in the range recommended by the supplier. Peroxidase labelled anti-rabbit and anti-mouse secondary antibodies was used for Western blot. Control experiments were done with each secondary antibody to detect possible non-specific cross-reactivity. Results were generally negative.

2.3 Methods

2.3.1 Immunofluorescence microscopy on isolated myofibrils

To measure the extensibility of titin domains in myofibrils, immunofluorescence microscopy was performed according to the following protocol. A drop of the myofibril suspension was placed on a glass coverslip under an inverted phase contrast microscope (Zeiss, Axiovert 135; Jena, Germany). Then, two glass microneedles were prepared using a horizontal micropipette puller and each glass needle was attached to a hydraulic micromanipulator (Narishige, Japan). A mixture of water-curing silicon glues, RTV3145 and RTV3140 (Dow Corning, USA), was prepared and, with the help of a third glass needle controlled by a mechanical micromanipulator, placed on the tip of the two other needles. The two glue-coated needle tips were then softly pressed against the ends of a desired myofibril specimen. After 5 min the ends of the myofibril were rigidly attached to the tips of the glass needles. At this point the rigor incubation solution was replaced by ATP containing solution (relaxing buffer) top help prevent structural damage from overly stretching the myofibrils.

Sarcomeric structures were visualized using a 100x oil-immersion objective (Plan Neofluar, Zeiss, Jena: numerical aperture 1.3). Myofibrils were examined for a regular striation pattern suggesting structural preservation and stretched to a desired SL. Phase contrast and fluorescence images were recorded with a CCD color video camera (Sony, AVT Horn).

The sample was incubated with appropriate concentrations of primary antibodies (typical dilution in relaxing buffer, 1:50 to 1:100) for ~30 min. Then the antibody solution was washed out with relaxing buffer (3 times wash) and the FITC or Cy3 conjugated secondary antibody was applied for another 30 min, before the specimen was washed extensively (initial volume of the solution exchanged ~4 times). Images were recorded in the epifluorescence mode of the microscope (example in Figure 11) using a 100 W arc lamp. Care was taken to minimize the exposure times to prevent extensive photo bleaching of fluorophores.

Figure 11. Typical experiment to determine segmental extensibility of I-band titin. A frog single cardiac myofibril was stained with an I-band titin antibody. The relative extension of the epitope to Z-line segment versus SL could be determined by measuring the closest distance between adjacent epitopes at different stretch states.

The distance between fluorescent epitopes was measured on digitized fluorescence images and the epitope position compared with the corresponding phase image, which was also used to measure SL. Because the epitopes appeared as relatively broad stripes (diffraction limit), the center-of-mass of the intensity signal was calculated from intensity profile plots along the myofibril axis (Linke et al., 1998 a). Data points obtained from many myofibrils were pooled into an epitope-distance versus SL diagram. The same procedure was repeated for other titin antibodies. The extensibility of a given titin segment was calculated by measuring the difference between the respective epitope-*versus*-SL curves.

2.3.2 Force measurements on myofibrils

A myofibril specimen was attached at one end to a force transducer and at the other end to the tip of a glass needle connected to a piezoelectric micromotor. Movement of the force transducer and gross displacement of the motor were controlled with the micromanipulators. Precise and rapid movements were imposed onto the specimen by controlling the piezoelectric motor, e.g., fast stretch-release oscillations to measure myofibrillar passive stiffness or a defined succession of stretch and hold steps followed by stepwise releases to measure passive force.

The principle of the force transducer is that an optical glass fiber is bent when a force is applied at the free end. As the ends of the specimen are glued to the micromotor and force transducer, respectively, movement of the motor needle at one end will induce changes in myofibrillar force which are transmitted to the force transducer. The end of the optical glass fiber is thus deflected and the deflection of this fiber (which is emitting white light) produces

a displacement of the light beam. This displacement is recorded by two receive optical fibers, whose light signal is transformed into electric current by a photodiode. Differential analysis of the two receive-fiber channels is done by an electronic module which transforms the two inputs into a single channel voltage signal (ΔV) proportional to the displacement, δ, of the emitting fiber tip. Knowing the Young's module, E ($\sim 7{,}7 \cdot 10^{11}$ mg/cm^2), for the glass fiber and the bending rigidity of the fiber, one can calculate the bending force, f, according to:

$$f = 3\delta \cdot E \cdot I / \text{ɬ}^3 , \qquad (2)$$

where ɬ is the length of the optical fiber and I is the geometrical moment of inertia, given by:

$$I = \pi \cdot d^4 / 64 \ . \qquad (3)$$

The relation between δ and ΔV is linear and should be established prior to each experiment by measuring the voltage change upon a known displacement of the optical fiber tip.

A National Instruments data acquisition board and custom written Labview software were used to control motor movement and data output and display and analyze (e.g., filter) the data. For details see Kulke et al. (2001 b). All force measurements on myofibrils were done in non-activating (relaxing) buffer in the presence of active-force suppressor, 2,3-butanedione monoxime, BDM. Passive tension was calculated by relating the force to the cross-sectional area of the specimen inferred from the myofibril diameter.

2.3.3 Proteolytic titin digestion by low-dose trypsin

To test whether titin is responsible for sarcomeric stiffness, specific proteolysis was performed using low concentrations (0.25 μg / ml) of trypsin. Trypsin is known to degrade almost all peptides, but at low enzyme concentrations muscle samples incubated with trypsin show rapid and dramatic, selective, titin degradation indicated by the appearance of a strong "T2" titin band on SDS-PAGE gels (presumed to be a proteolytic product of native titin). In contrast, bands for other muscle proteins seem to be unaffected by mild trypsin digestion (Cazorla et al., 1999). Rapid loss (within 3 to 10 min) of myofibrillar passive tension was observed during trypsin treatment (0.25 μg/ml in relaxing solution) (Kulke et al., 2001 b).

2.3.4 Immunofluorescence microscopy on tissue sections

In situ examination of muscle proteins was done by immunofluorescence microscopy on tissue sections fixed with paraformaldehyde (PFA). Procedures for immunofluorescence

on tissue sections were performed using PBS solutions. Muscle fibers were incubated on ice in PBS containing 4% PFA overnight and were then transferred to 10% sucrose solution (4°C) for 24 hours. Thin sections (20 μm thick) were cut at –20°C and stored in PBS on ice.

A standard protocol for tissue immunofluorescence microscopy was applied (modified from Antohe et al., 1999). Briefly, sections were incubated for 10 min in PFA-Tx, 10 min in 50 mM NH_4Cl, 10 min in 2%BSA / PBS-Tx, and then 2 h with primary antibody (in 2% BSA / PBS). Sections were washed 3 x 10 min with PBS-Tx, then incubated for 2 h with the fluorescently labelled secondary antibody and washed 3 x 10 min. The section in PBS-glycerol was placed on a glass slide and a cover slide was put on top. The specimen was examined under the inverted fluorescence microscope (Zeiss Axiovert 135) and images were recorded by the CCD color camera as noted above.

2.3.5 Sample solubilization and protein concentration measurements

Tissue strips (~1 cm long and 3 mm wide) were cut from frozen ventricle and immediately put in 1.5 ml reaction tubes with ice cold solubilization buffer. Samples were boiled (100°C) for 3 min, then centrifuged for 3 min at 16 000 x g. Approximately 2 μl of sample were taken to determine the protein concentration.

The total protein content of the samples was analyzed spectrophotometrically using the Bradford method (BioRad Protein Assay) according to instructions by the supplier. Absorbance was read at 595 nm wavelength and protein concentration was calculated from the optical density using a standard curve as reference. For titin analysis, optimal protein loading on gels was 50-80 μg / lane.

Myofibrillar fraction assay. Muscle pieces were homogenized in 50 μl relaxing buffer. Subsequently 1 ml relaxing buffer was added, the sample was centrifuged and the supernatant placed in a separate tube for TnI western blot analysis. SB-buffer was then added to the pellet and supernatant.

2.3.6 SDS polyacrylamide gel electrophoresis

Standard polyacrylamide gels were prepared by the protocol of Laemmli (1970). Gels with various acrylamide concentrations (from 1.8% to 18%) and sometimes gels with a concentration gradient were made.

2.3.6.1 Titin detection on 2% SDS-polyacrylamide gels

Large MW proteins, like titin, need a low porosity gel matrix in order to run a measurable distance in the electric field. However, these gels are very fragile. Tatsumi and Hattori described in 1995 a method to give mechanical strength to low porosity gels by adding agarose (0.5%) to the gel components. In the present work the Biometra Minigel-Twin system (Biometra biomedizinische Analytik GmbH, Göttingen) was used to study titin by gel electrophoresis. The design is optimized for separation of proteins in vertical 8.6 x 7.7 cm gels. The glass plates have fixed spacers and the sealing is obtained with one-piece silicone rubber seals.

Pre-warmed (50°C) gel solution (AA-BA) was mixed (for recipe see section 2.4 Solutions) and agarose (1.5% stock) was boiled in the microwave oven. Appropriate volumes of agarose and acrylamide-bisacrylamide solution were mixed to reach the desired agarose concentration. APS was added and the mixture was quickly loaded to the moulds of the gel chamber. Immediately thereafter a comb to form the loading pockets was put on top of the gel, which was left to polymerize for a minimum of 2h at 4°C. The final agarose concentration, which determines the mechanical properties of the gel, varied between 0.4% and 1%. Acrylamide concentrations ranged from 1.8% to 2.8%, the latter was used to visualize titin and myosin heavy chain (MHC) on the same gel.

After polymerization the gel was placed in the running chamber, and the solubilized samples were loaded (2-18 μl per lane). The best separation for the high molecular weight proteins was obtained by running the electrophoresis overnight at 2 mA per gel. Gels were then taken out from the glass mould and stained by Coomassie blue for 1 h using staining solution (coomassie blue dye, 40% methanol, then 10 min in 50% ethanol / 7% acetic acid, and 2-4 h in 5% ethanol / 7% acetic acid. Silver staining was performed with Bio-Rad Silver Stain Kit (Bio-Rad Laboratories, USA) according to the recommended protocol. Gels were scanned wet and dried on paper or between cellophane foils using a Biometra Gel-Dryer system.

Calibration of titin gels. To estimate the molecular weight of a protein by gel electrophoresis one typically uses molecular weight (MW) markers and an interpolation method. The method does not work for titin, as there are no commercial MW markers available in this size range. The assumption for 2% polyacrylamide gels is that the running distance increases exponentially as the molecular weight of the protein decreases (Wang and Wright, 1988; Wang et al., 1991; Granzier and Irving, 1995). Calibration can be done using titin and nebulin

with known MW size as reference markers. For instance, rabbit soleus titin has a molecular weight of 3.6-3.7 MDa, whereas rat heart expresses almost exclusively the ~3.0 MDa N2B-titin isoform. Rabbit nebulin is around 750 kDa.

Although titin and MHC could be visualized on 2.8% polyacrylamide gels on the same gel lane, the huge size difference between the two proteins made a determination of the molar ratio difficult, as the stainability of these proteins is different (Neuhoff, 1990). Nevertheless, the molar ratio between MHC and titin could be calculated with reasonable precision, suggesting 3 to 6 titin molecules are present per half thick filament (Liversage et al., 2001). A substantial effort was made to quantify titin expression in samples from diseased and normal muscles (Neagoe et al. 2002, Wu et al. 2002, Anderson et al. 2002, Hunter et al. 2003).

2.3.6.2 SDS-polyacrylamide gradient gels

High AA-BA and low AA-BA concentration solutions were prepared (see 2.4 Solutions) to make polyacrylamide gradient gels. The gradient forming device consisted of two tubes communicating through a pipe located at their bottom. One of the tubes had another pipe at its bottom side to let the mixture of acrylamide solutions flow into the gel mould. All pipes had valves with an open-closed mode of operation. Each acrylamide solution was put in a tube of the mixing chamber, stirred, and APS was added to each tube. The valve between the tubes was opened, then the outflow valve was opened and the gel mould filled with the solution from the mixing chamber. Because of the density gradient, the solution with a high AA-BA concentration flows faster and is deposited at the bottom of the gel. The low AA-BA concentration solution was mixed with the high AA-BA concentration solution and the solutions passed from one chamber to the other via the communicating tube. The result was a gradient in AA-BA concentration increasing from the top to the bottom of the gel.

2.3.6.3 Gel image acquisition and analysis

Digital pictures of the stained gels were taken using a through-light scanner (Scanmaker E6, Microtek) in the "positive transparency" scanning mode. Optimum scanning resolution was considered to be 600 dpi on a 256 greyscale. Optical volumes (OVs) of the

bands were calculated using TotalLab software (TotalLab, Phoretix, USA). MW size was estimated using an algorithm in which a logarithmic relationship between running distance and MW was assumed.

2.3.7 Western blot

Western blotting was employed to identify the titin isoforms, cTnI, MHC, and desmin. The SDS-PAGE gel, PVDF membrane and pieces of Whatman paper were rinsed in ice cold TB. Then a sandwich consisting of paper, gel, PVDF membrane, and again paper, was built and put in a transfer tank with TB. The setup was connected to a DC power source. The time and the electric parameters for the protein transfer depended on the molecular weight of the band to be transferred: the larger the protein, the higher the charge for transfer (Q), where Q = i * t is the product of current intensity and transfer time. For titin, an optimal transfer was achieved at 700 mA for 6h. Active cooling was used to dissipate excessive heat.

After electrotransfer, the membrane was washed 2 x in TBS-Tx. Then it was checked by Poinceau red staining whether protein bands were present on the membrane. Poinceau solution was washed away with TBS and the membrane was incubated for 2 h with 2% BSA / TBS solution to block unspecific binding sites. Procedures were done at room temperature. The primary antibody incubation time was 1h in BSA / TBS buffer. Then, the membrane was washed 1 x 15 min + 2 x 5 min with TBS, incubated for 30 min with the secondary peroxidase-conjugated antibody (dilution 1:70,000 in TBS-Tx; Sigma-Aldrich) and washed 1 x 15 min + 3 x 5 min. Incubation with the secondary peroxidase-conjugated antibody only was done as a control to test for non-specific primary antibody reaction.

Chemiluminescent assay. Visualisation of the protein bands on the blot membrane was done using the light emitted when luminol is oxidized by H_2O_2, a reaction catalyzed by peroxidase. For the present work I used an ECL chemiluminescent kit (Amersham Pharmacia biotech). It consists of two solutions mixed in equal volumes just before use. Chemiluminescent reaction was recorded on autoradiography film (Kodak X-Omat XAR 5; manoeuvre performed under red light) in an autoradiography cassette. After one, three, or ten minutes, the film was removed, developed, fixed (Kodak kit) and dried. The picture was scanned and analysed in the same way as described for gels.

In some experiments it was necessary to test different antibodies on the same membrane. To do so, the bound antibodies were stripped off by incubation with reprobing buffer for 30 min at 50°C.

2.3.8 Force and shortening velocity measurements on muscle fibers

Passive and active isometric force or maximum unloaded shortening velocity (according to Edman, 1979) were measured in skinned cardiac trabeculae or psoas muscle fibers obtained from freshly excised rat or rabbit hearts and skeletal muscle.

The diameter and the length of the fibers were measured under a binocular microscope. Usual dimensions were 0.15-0.4 mm (thickness) by 2-4 mm (length). In a typical experiment the ends of a skinned fiber were attached via miniature stainless steel tweezers to a force transducer and a linear moving motor (Muscle Research System apparatus; Scientific Instruments, Heidelberg) (Figure 12). Custom written software (thanks to Mr. Uros Krzic) was used to drive the apparatus in stretch (release)-force acquisition protocols. Nonactivated specimens were slowly stretched to a desired SL. Sarcomere length was measured by laser diffraction using a laser diode emitting at a wavelength of 670 nm. The fiber bundle was left to equilibrate for 5 min in the equilibration solution 1, then the preparation was transferred to activating solution.

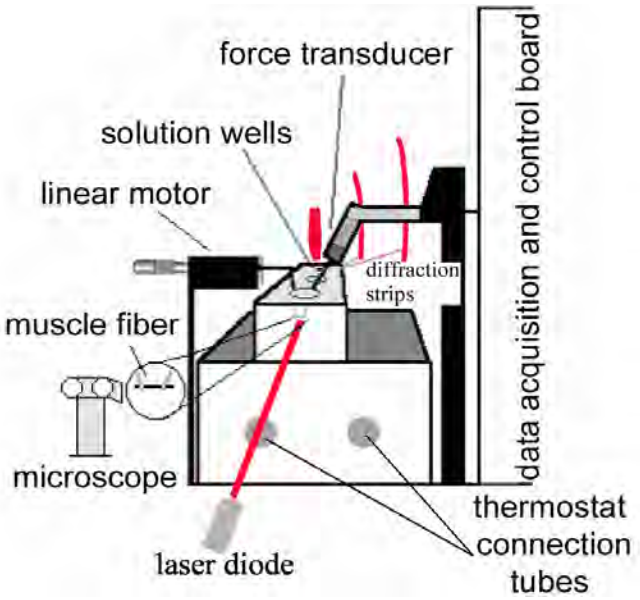

Figure 12. Experimental setup for isometric force, isotonic shortening and slack test measurements. The muscle fiber was attached via miniature stainless steel tweezers to a linear motor and a force transducer. Length and diameter of the specimen were measured under a binocular microscope. Sarcomere length was determined by laser diffraction. The wells contained various solutions with different Ca^{2+} concentrations.

2.3.9 Isolation and culture of adult rat cardiomyocytes

Female Sprague-Dawley rats (2-month old) with a body weight of 200-220 g were anesthetized and the heart was excised. Then the heart was perfused retrogradely via the aorta with Joklik medium (gassed with a 5% CO_2 : 95% O_2 mixture) for about 10 minutes. The perfusion continued for another 35 min with Joklik medium containing collagenase 2 (see 2.4 "Solutions"). The heart was cut off below the atria and chopped into fine pieces, then washed with "Kraftbrühe" solution (see 2.4 "Solutions"). The tissue was further treated with collagenase / Kraftbrühe solution in a 37°C water bath under shaking. The digested tissue was carefully pressed through a Nylon filter and the resulting cell suspension centrifuged. The pellet of cells was transferred to Joklik medium containing 0.5 mM $CaCl_2$, mixed and again centrifuged.

Cells were recovered as pellet and cultured for 2 h in M199 medium (Gibco) + 5 mM creatine at 5% CO_2 atmosphere, 37°C, then the cell suspension was centrifuged and recultured in medium M199 supplemented with serum (10%), antibiotics (1%), and cytosine arabinoside (see 2.4 "Solutions"). The culture plates had previously been coated with collagen R (Serva) according to the manufacturer's recommended protocol. After 2 days the medium was exchanged and such medium exchange was repeated every 5 days as described (Eppenberger-Eberhardt et al., 1997).

2.4 Solutions

2.4.1 Solutions for immunofluorescence microscopy on tissue sections

<u>Phosphate Buffered Saline (PBS)</u>

16 g NaCl, 0.4 g KCl, 3 g Na_2HPO_4 * $2H_2O$, 0.4 g KH_2PO_4

<u>Paraformaldehyde / glutaraldehyde fixation solution (PFA / GA)</u>

Paraformaldehyde (4%) was dissolved in H_2O by stirring and heating to 50-60°C. Then the solution was clarified with several drops of 1 M NaOH and the pH adjusted to 7.1 using HCl. Aliquots of 10 ml were prepared and frozen at -20^0C. Optionally, 0.8% glutaraldehyde could be added just before use.

2.4.2 Solutions for muscle fiber preparation and myofibril mechanics

Rigor solution 1 ("extracellular")

132 mM NaCl, 5 mM KCl, 7 mM glucose, 1 mM $MgCl_2$, 4 mM TES, 5 mM EGTA, pH 7.1 (adjusted with KOH).

Rigor solution 2 ("intracellular")

75 mM KCl, 10 mM Tris, 2 mM $MgCl_2$, 2mM EGTA, 40 μg/ml leupeptin, pH 7.1 (adjusted with KOH).

Relaxing solution pCa 9.2

9.2 mM Mg-methanesulfonate, 12 mM K-methanesulfonate, 3.2 mM Mg-ATP, 130 mM MOPS, 15.5 mM EGTA, 40 μg/ml leupeptin (Peptide Institute, Osaka, Japan), pH 7.1 (adjusted with KOH).

Equilibration solution 1

20 mM imidazole; 2 mM EGTA; 10 mM $MgCl_2$; 7.5 mM ATP; 1 mM NaN_3; 10 mM creatine phosphate, pH 7.0 (adjusted with KOH).

Activating solution pCa 4.5

20 mM imidazole; 2 mM EGTA; 10 mM $MgCl_2$; 7.5 mM ATP; 1 mM NaN_3; 10 mM creatine phosphate, 4 mM $CaCl_2$ (pCa 4.5), pH 7.0 (adjusted with KOH).

2.4.3 Solutions for SDS-PAGE

Standard x % separation gel (Laemmli)

A desired amount (x %) (w/v) acrylamide mixture (30:0.8 acrylamide : bisacrylamide), 375 mM Tris (pH 8.8), 0.1% (w/v) SDS, 0.005 (v/v) TEMED, then 0.05% (w/v) APS added to start the polymerization. An example is as follows:

8%-gel, volume for 2 minigels

stock solution		volume
Acrylamide : bisacrylamide	(30% / 0.8%)	4 ml

Glycerol : H_2O	0.75 ml
Lower Tris (1.5 M Tris, 0.4% SDS, pH 8.8)	3.75 ml
20% SDS	0.1 ml
H_2O	6.4 ml
TEMED	7.5 µl
10% APS	75 µl

Concentration (stacking) gel 3%

3% (w/v) acrylamide, 125 mM Tris (pH 6.8), 0.1 % (w/v) SDS, 0.02% (v/v) TEMED, then 0.6% (w/v) APS added to start the polymerization.

Gradient gels

1.8 to 10% gradient, volume for 2 minigels

"1.8%" solution (take 4 ml / gel)

stock solution	volume
Acrylamide : bisacrylamide (30% / 0.8%)	0.54 ml
Lower Tris (1.5 M Tris, 0.4%SDS, pH 8.8)	4 ml
H_2O	4.38 ml
TEMED	5 µl
10% APS	18 µl

"10%" solution

stock solution	volume
Acrylamide : bisacrylamide (30% / 0.8%)	2.67 ml
Glycerol : H_2O (1:1 v/v)	1 ml
Lower Tris (1.5 M Tris, 0.4% SDS, pH 8.8)	4 ml
H_2O	0.29 ml
TEMED	3.75 µl
10% APS	18 µl

10 to 18% gradient, volume for 2 minigels

"10%" solution (take 4 ml / gel)

stock solution	volume
Acrylamide : bisacrylamide (30% / 0.8%)	5.52 ml
Lower Tris (1.5 M Tris, 0.4% SDS, pH 8.8)	4 ml
Glycerol : H_2O (1:1 v/v)	1.2 ml
H_2O	5.52 ml
TEMED	8 µl
10% APS	18 µl

"18%" solution (take 3.5 ml / gel)

stock solution	volume
Acrylamide / bisacrylamide (30% / 0.8%)	9.6 ml
Glycerol	2.4 ml
Lower Tris (1.5 M Tris, 0.4% SDS, pH 8.8)	4 ml
TEMED	8 µl
10% APS	18 µl

Low acrylamide concentrations (1.8% to 2.8%) in agarose-strengthened gels

For 0.5% (w/v) agarose, stock 1.5% is melted and an appropriate amount is mixed with AA-BA solution. For AA-BA solution, 2% (w/v) acrylamide (30 : 0.8), 375 mM Tris (pH 8.6), 0.1% (w/v) SDS, 0.075% (w/v) APS, 0.06% (w/v) TEMED are mixed. Examples are as follows:

***2% gel*, volume for 2 minigels**

stock solution	volume
Acrylamide : bisacrylamide (30% / 0.8%)	1.3 ml
Lower Tris (1.5 M Tris, 0.4% SDS, pH 8.8)	5 ml
20% SDS	0.1 ml
H_2O	5.9 ml
TEMED	11.5 µl

The mixture is prepared in a 50 ml plastic tube, warmed to 50°C, and the following is added:

10% APS	0.150 ml
1.5% agarose (melted in a microwave oven)	6.65 ml

***2.8% gel*, volume for 2 minigels**

stock solution	volume
Acrylamide : bisacrylamide (30% / 0.8%)	1.533 ml
Lower Tris (1.5 M Tris, 0.4% SDS, pH 8.8)	5 ml
20% SDS	0.1 ml
H_2O	4 ml
TEMED	11.5 µl

The mixture is prepared in a 50 ml plastic tube, warmed to 50°C, and the following is added:

10% APS	0.150 ml
1.5% agarose (melted in a microwave oven)	5 ml

Running buffer

25 mM Tris (pH 8.3), 192 mM glycine, 0.1% (w/v) SDS

Sample solubilization buffer

4.3 mM Tris, 4.3 mM EDTA, 1% SDS, 1% 2-mercaptoethanol, 10% (v/v) glycerine, 0.1% (w/v) bromophenol blue, 4 µg/ml leupeptin

Staining solution

0.1% (w/v) Coomassie Brilliant Blue G250, 7% (v/v) acetic acid, 40% (v/v) methanol.
The recipient is covered, the solution is stirred for more than 2 h, and then filtered.

Destaining solutions (in v/v)

a) 50% ethanol, 7% acetic acid

b) 5% ethanol, 7% acetic acid

2.4.4 Solutions for electrotransfer and Western blot procedures

Transfer buffer (TB)

25 mM Tris (pH 8.3), 192 mM glycine, 0.1% (w/v) SDS, 15 % methanol

Tris Buffered Saline (TBS)

50 mM Tris HCl, 150 mM NaCl, pH 7.3

To obtain a blocking buffer for Western blot incubations, optionally add:

0.05% Triton X-100

2% bovine serum albumin

Antibody stripping buffer

100 mM 2-mercaptoethanol, 62.5 mM Tris-HCl (pH 6.8) 2% SDS, pH 6.7 (HCl-adjusted).

2.4.5 Solutions for cardiomyocyte isolation and cell culture

All solutions have to be sterile filtered or autoclaved (where possible).

"Kraftbrühe" (KB) solution (according to Isenberg and Klöckner, 1982)

70 mM KCl, 30 mM K_2HPO_4 , 3.96 mg/ml glucose, 1.22 mg/ml $MgSO_4$ * $7H_2O$, 0.5 mM EGTA, 2.5 mg/ml taurine, 0.65 mg/ml creatine, 0.22 mg/ml pyruvic acid sodium salt, 10 mM succinate, 5 mM Na-ATP * $5H_2O$, 2 mM 2-hydroxy-butyric acid, pH 7.4 (adjusted with KOH), filter sterile.

Joklik medium

1 package of Joklik powder (Sigma-Aldrich) is dissolved in water and the following supplements are added: 30 mM taurine, 1 mM adenosine, 26 mM $NaHCO_3$, 2.5 mM L-glutamic acid. The solution is stirred for 1 h under gassing (O_2:CO_2 mixture, 95:5%), pH adjusted to 7.1 (with NaOH or HCl), and the medium is then sterile filtered.

Collagenase solution

For one isolation procedure 120 units/ml collagenase type 2 (Worthington) are dissolved in 50 ml Joklik medium for the perfusion solution and 60 units/ml in 20 ml KB solution. Collagenase solutions should be prepared before use because of autolysis of the enzyme.

M199 – cell culture medium

Medium was used supplemented with 20 mM creatine, 1% penicillin / streptomycin, 10 μM cytosine arabinoside, 10% fetal calf serum.

2.5 Statistical analysis

Data were analysed using the Student's t-test with $p<0.05$ as a criterion for statistical significance. Data were expressed as mean ± SEM (standard error of the mean), if not indicated otherwise.

3. RESULTS

3.1 Cardiac and skeletal titin expression investigated by gel electrophoresis

3.1.1 The ratio between cardiac titin isoforms is not significantly affected by titin degradation

Expression of the major titin isoforms (N2B and N2BA) in human myocardium was quantified by low percentage SDS-PAGE. Various acrylamide concentrations (1.8% to 2.8%) were used in agarose strengthened gels. 2.8% polyacrylamide gels separated MHC from titin and, with low resolution, cardiac titin isoforms, N2B and N2BA (Figure 13). The ratio between proteins appearing on gels was calculated from the calibrated OV of the bands. The results were presented either as the ratio between the OV of the bands or as a percentage like:

$$N2BA\,(\%) = \frac{N2BA}{N2B + N2BA} \times 100 \qquad (4)$$

For an appropriate quantitation of the OV ratio of the bands, a calibration procedure was necessary, since the gel bands of different proteins could have different stainability: the porosity of the gel (determined by the polyacrylamide concentration) is a factor that influences the protein staining properties of the coomassie dye (Neuhoff et al., 1990). Hence, the data included in the statistics on protein expression ratio were usually obtained from the same gel type. Also, the range of protein loading on a gel lane within which the OV increases linearly is limited. Therefore, “calibration gels" were generated to measure the relationship between the amount of total protein loaded on lanes and the expression ratio for proteins.

On 2.8% SDS-PAGE gels, protein load did not significantly affect the N2BA:N2B titin-isoform ratios, in the range from 20 to 70 μg per lane (Figure 13). Titin isoform ratios were similar to those determined on 2-10% polyacrylamide-gradient gels. The titin : MHC ratio on 2.8% gels was constant at loads >55 μg/lane (Figure 13) but was generally lower (≤0.1) than that seen on 2-10% polyacrylamide gradient gels (~0.21); the latter value has also been reported in the literature (Granzier and Irving, 1995; Liversage et al., 2001). The differences in the titin : MHC ratio thus arise from the usage of different gel types. No effort was made to further explore possible reasons for these differences.

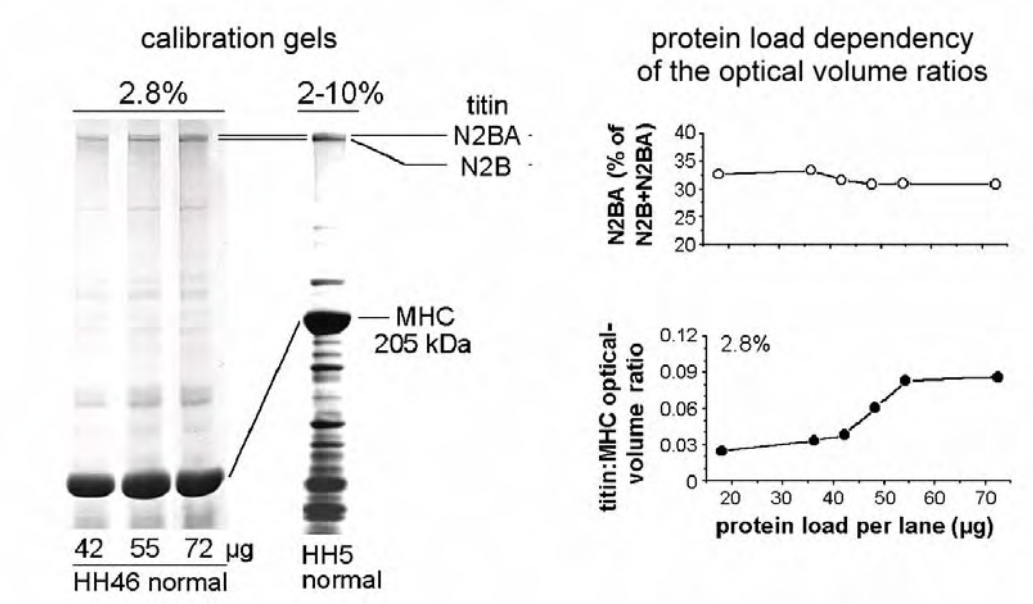

Figure 13. SDS-PAGE calibration gels to determine the relationship between ratios of optical volume (band intensities) and protein loading. For titin, the N2BA proportion is relatively constant for a large range of protein loadings, whereas the apparent titin:MHC ratios are highly dependent on protein load (and gel concentration).

Titin is well known to be rapidly cleaved by very low amounts of trypsin. Incubation of myofibrils with low-dose trypsin was reported to leave intact all other sarcomeric proteins except titin (Cazorla et al., 1999). An explanation for this effect may be the easy accessibility of the enzyme to degradation sites facilitated by the long extended shape of the titin molecule. Also, the number of cleavage sites may increase with the dimension of the polypeptide, which would explain the high susceptibility of titin molecules to trypsin compared with other proteins. In the case of titin, larger isoforms might be affected more rapidly by trypsin than shorter isoforms.

A sign of titin degradation is considered to be the appearance of T2-bands (MW, 2300-2500 kDa) on SDS-PAGE gels. We addressed the possibility that differences in measured titin isoform ratio arise from a different susceptibility of the isoforms to degradation (Figure 14). A normal human-heart sample was allowed to degrade at room temperature in the absence of leupeptin. The intensity of T2, the titin-degradation band, rapidly increased, whereas the N2BA:N2B ratio initially remained unaltered and was reduced only after 30 to 60 minutes of degradation. We conclude that under "normal" study conditions (*i.e.*, in the presence of leupeptin, which largely prevents appearance of T2), the measured N2BA:N2B ratio is independent of possible minor protein degradation processes.

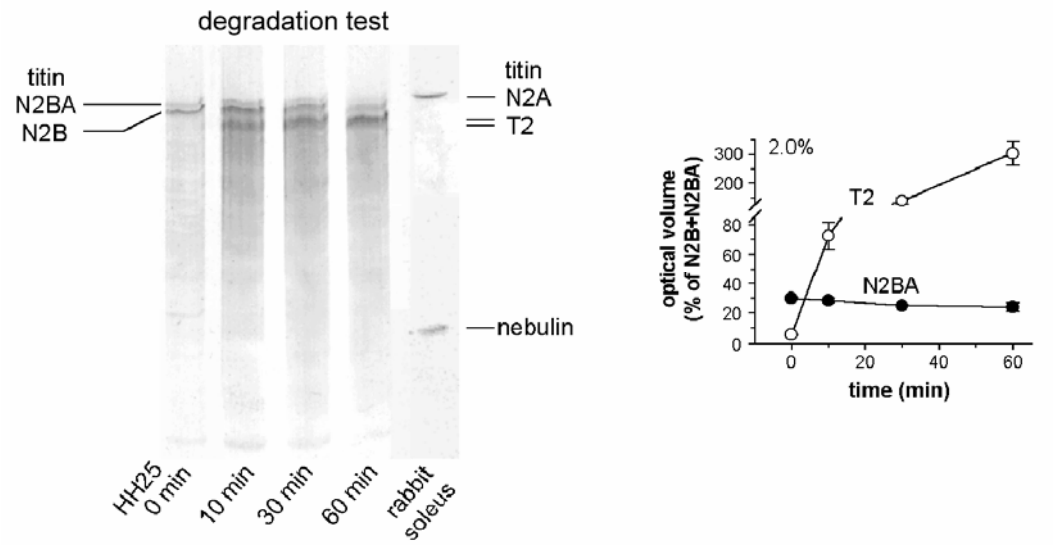

Figure 14. Assessment of titin degradation. Tissue samples were left to degrade at room temperature in the absence of protease inhibitor (leupeptin). After 10 minutes, strong T2 bands (titin degradation products) appeared and the intensity of the native titin bands decreased, without a significant change in N2BA:N2B ratio. Symbols are mean ± SEM (n=6).

3.1.2 Multiple isoforms are visible within the N2BA-titin band

The best separation of titin bands was obtained using 1.8% SDS-polyacrylamide gels (Figure 15). Typically, rabbit soleus muscle and normal rat heart showed a sharp band at 3600-3700 (N2A isoform) and 3000 kDa (N2B isoform), respectively. In contrast, a human heart sample exhibited both a sharp N2B band and a wide N2BA-titin band (3300-3500 kDa), suggesting the presence of multiple N2BA isoforms.

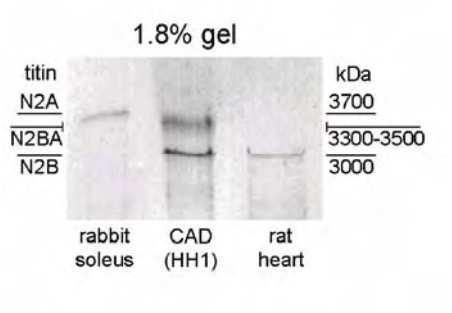

Figure 15. 1.8% SDS-PAGE gel used to determine titin isoform expression in rabbit soleus, human heart and rat heart tissue. N2A and N2B titin were sharp bands, whereas N2BA-titin appeared as a spectrum of isoforms with various molecular weights from ~3300 to 3500 kDa.

To confirm the identity of the bands we employed Western blotting after running 2% SDS-PAGE titin gels. Antibodies to both N2B and N2BA titin were used. Staining of N2BA titin using MG1 antibody (to N2-A domain) was frequently stronger in CAD and DCM hearts than in normal hearts. Both isoforms were visualized by reprobing the same membranes with BD6 antibody (stains near the I-band/A-band junction) (see Neagoe et al., 2002).

3.1.3 Co-expression of cardiac titin isoforms occurs at the sarcomere level

Titin provides an elastic link between the Z-disc and the M-line of the sarcomere. A variable combination of functional modules in I-band titin (Ig domains, PEVK and N2B segments) gives rise to a large variety of muscle-specific titin isoforms. As mentioned above, cardiomyocytes co-express two major titin isoforms, N2B and N2BA, in the same sarcomere. Co-expression of different length titin isoforms in a sarcomere is a way to adjust myofibrillar passive stiffness (Linke et al., 1999). In the experiment of Figure 16, a human cardiac myofibril was stained with two different antibodies, to N2-B domain (N2B) and to N2-A domain (MG1). The MG1 antibody stained in a regular double-striated pattern showing the presence of N2BA titin in all sarcomeres. There were no myofibrils/sarcomeres detected that did not stain positive for the N2BA isoform (also see Neagoe et al., 2002).

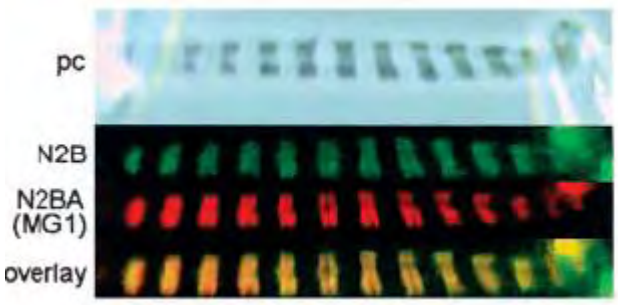

Figure 16. Titin expression in human cardiac myofibril by immunofluorescence microscopy using epitope-specific antibodies. Both N2B and N2BA titin are stained by N2B-antibody, whereas N2BA is stained only by MG1. The two epitopes co-localize in all sarcomeres and move together during stretching (myofibril mechanical manipulation by Dr. Michael Kulke).

3.1.4 Analysis of titin isoform size and composition by gel electrophoresis

Cardiac titin isoform ratio varies between species, following a trend in which small mammals like rats express almost exclusively N2B titin, whereas in the myocardium of cows

or pigs the N2BA-isoform predominates or is at least as abundant as the N2B-isoform (Cazorla et al., 2000). As the body weight of a mammal seems to correlate well with the heart rate (Lindstedt et al., 2002), there may also be a direct relationship with the cardiac titin isoform ratio. On the other hand, it was reported that titin isoform composition varies substantially in one and the same heart (Cazorla et al. 2000): the right atrium of pig and cow expresses relatively more N2BA than the left ventricle. Additional variation in N2BA:N2B-titin ratio is seen between sub-epicardial, midwall, and sub-endocardial tissue.

A systematic assessment of cardiac titin-isoform expression and composition was performed in several species using high resolution 2% SDS polyacrylamide gel electrophoresis (Figure 17). The main results of these studies were as follows:

a) The MW of N2B cardiac-titin isoform was similar in all mammalian species investigated, around 3000 kDa.

b) The molecular size of the adult N2BA-titin isoform(s) was between 3200 and 3400 kDa, in agreement with the sizes expected from sequence analysis (3200-3350 kDa; Freiburg et al., 2000); these isoforms are likely to represent full length titin molecules.

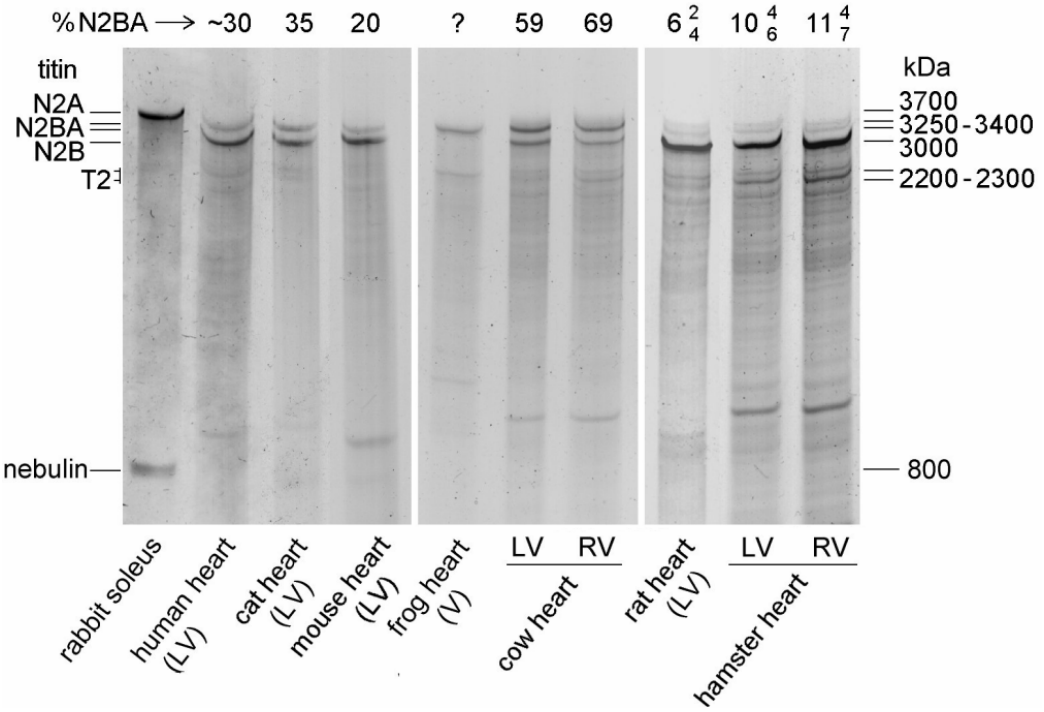

Figure 17. Cardiac titin isoforms in different species. Multiple N2BA-titin bands were identified in a MW range from 3.2 to 3.4 MDa. N2BA:N2B ratio varied considerable from almost exclusively N2B in rat heart up to ~70% N2BA in cow RV. The respective N2BA proportion (% of N2B + N2BA) is indicated above each lane (from Neagoe et al., 2003).

c) The N2BA:N2B titin ratio varies considerably between species and is not strictly related to heart mass, heart rate or body size. The N2BA-titin percentage in the LV increased in the following order: rat < hamster < rabbit (not shown here) < mouse <sheep < human < cat < pig (not shown) < goat < cow.

d) The N2BA : N2B titin ratio varies between the LV and the RV of the same animal (this comparison was made in hamster, rabbit, sheep, goat, and cow heart); RV was found to always have higher ratios than LV.

e) In some species (e.g., rat, hamster) the cardiac N2BA-titin band appeared as a clear doublet, or even a triplet in pig RV (data not shown). The MW of the doublets was 3200-3400 kDa in rat and hamster and 3400-3500 kDa in cow. The two N2BA bands were best detected when the gels were loaded with sufficient amount of protein and destained modestly. A doublet N2BA-titin band had been previously reported for bovine left atrium (Trombitas et al., 2001).

f) There is some correlation between the resting heart rate of a mammalian species and the titin isoform ratio. However, some species do not fit in this trend, e.g. mouse has about 20% N2BA titin but a faster heart rate than rat, which has less than 10% N2BA titin.

g) Frog ventricle expresses a single titin isoform of ~3300 kDa MW. Antibody staining suggested that some of the mammalian titin epitopes are present in frog heart titin, whereas others are missing. The identity of this frog cardiac titin band (N2B, N2BA, N2A or other) remains to be determined.

h) T2-bands, considered to be proteolytic products of intact titin, were quite faint on these gels, indicating that the tissue preparation procedure resulted in only minor titin degradation and that the method used for quantitation of titin isoform ratio is reliable.

The titin gel information was used to quantify the titin expression ratio in human heart samples. To do so, an intensity profile crossing the titin bands perpendicularly was recorded and parameterized using a three-Gaussian fit, where a one-Gaussian described the N2B peak and the sum of two Gaussians the broad N2BA signal (Figure 18). In Makarenko et al. (2004) and Opitz et al. (2004), the parameters obtained from such fits were used to predict titin-based stiffness, by also considering the parameters of titin elasticity determined by single-molecule mechanics (Li et al., 2002).

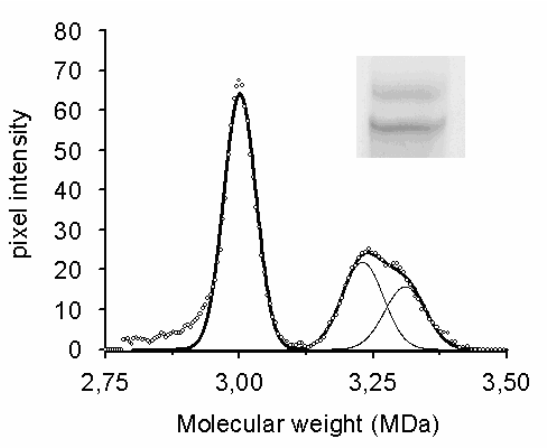

Figure 18. Average intensity profile (open circles) of cardiac titin bands separated on 2%-gel lanes (a typical lane is pictured as inset; profiles of from 7 human DCM were included in the analysis). Assuming that the band that represents a titin isoform appears on gel as a Gaussian distribution of the staining intensity, the experimental curve of the N2BA-titin band is fitted as a sum (thick line) of two Gaussians. A doublet N2BA-titin band is suggested (the mathematical fit was performed by Dr. Mark Leake).

3.1.5 Topology of cardiac titin isoform composition in normal adult hearts

Previously it was reported that the N2BA:N2B isoform ratio differs in sub-epicardial tissue versus sub-endocardial tissue (Cazorla et al., 2000). This issue was studied in the cardiac walls of normal adult human, sheep, goat, rabbit and pig hearts. However, no significant transmural differences in the N2BA:N2B ratio were found, although in the hearts of larger species like goat there was a trend towards increased N2BA proportions in the endocardium, compared to the epicardium (Figure 19). In contrast, there was substantial heterogeneity of titin isoform composition across the heart chambers. The apex expressed relatively less N2BA titin than the heart basis (Table 1 and Figure 19). The interventricular septum showed an N2BA:N2B ratio in between that of the apex and basis. The RV had a higher N2BA percentage than the LV.

Particular attention was paid to the situation in human left ventricle (non-failing donor hearts). The possibility of a transmural gradient in N2BA:N2B ratio was investigated using sub-endocardial, mid-wall, and sub-epicardial LV tissue from altogether 9 donor hearts (Figure 20). However, no transmural gradient of titin isoform ratio could be detected.

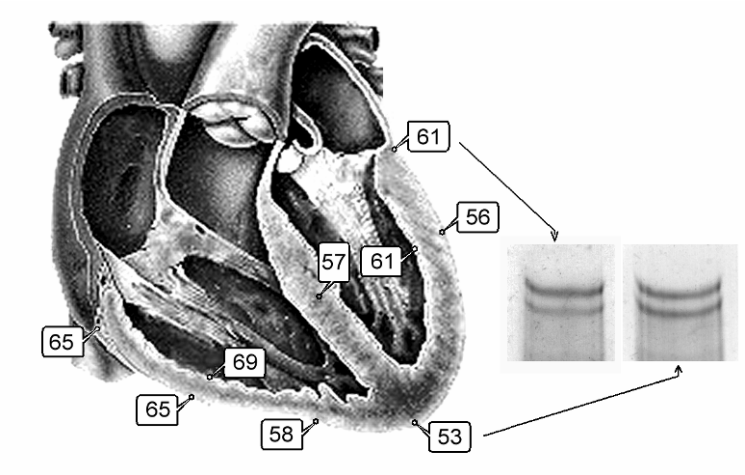

Figure 19. Topology of N2BA:N2B-titin isoform ratio in the heart of a goat. The right ventricle has a higher relative N2BA expression than the left ventricle. The N2BA:N2B ratio decreases from the basis to the apex.

Table 1. Results of 2% SDS-PAGE analyses of goat heart tissue. Percentage of N2BA titin (relative to N2B+N2BA, which is 100%) is presented as mean ± SD (number of lanes analyzed). No/yes indicates whether there are statistically significant differences between the samples from different regions of the heart, at the $p<0.05$ level (unpaired Student's t-test). LV: left ventricle; RV: right ventricle; Epi: sub-epicardium; Endo: sub-endocardium; mid: mid-wall.

	LV, epi, basal	LV, epi, equatorial	LV, endo, equatorial	Septum, mid, equatorial	RV, epi, basal	RV, epi, equatorial	RV, endo, equatorial	RV, epi, apical	Apex, epi
LV, epi, basal	61±2 (6)								
LV, epi, equatorial	no	56±3 (5)							
LV, endo, equatorial	no	no	61±1 (4)						
Septum, mid, equat.	no	no	yes	57±1 (4)					
RV, epi, basal	yes	yes	no	yes	74±4 (5)				
RV, epi, equatorial	no	yes	no	yes	yes	65±2 (8)			
RV, endo, equatorial	yes	yes	yes	yes	no	no	69±1 (6)		
RV, epi, apical	no	no	no	no	yes	yes	yes	58±1 (7)	
Apex, epi	yes	no	yes	no	yes	yes	yes	no	53±3 (5)

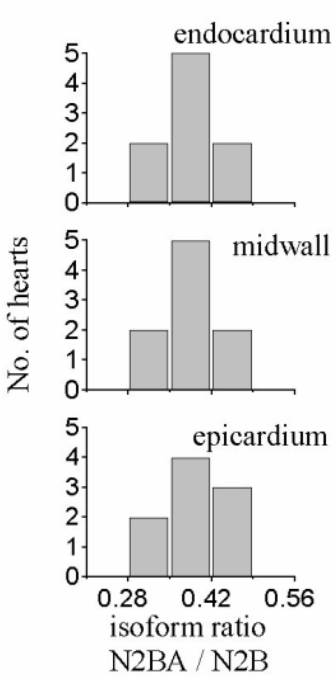

Figure 20. N2BA:N2B titin ratio assessed in human LV across the ventricular wall in the medial plane. Titin isoform ratio did not vary significantly from the sub-epicardial to the sub-endocardial region; the variation in N2BA-titin percentage was less than 5%.

3.2 The N2BA:N2B isoform expression pattern is altered in diseased hearts

3.2.1 Increased N2BA:N2B titin ratio in hearts of coronary artery disease patients

Myocardial samples from human patients with coronary artery disease (CAD) were investigated for their titin isoform pattern, in comparison to non-ischemic transplants and non-failing human donor hearts. The average N2BA proportion of individual HHs is shown in Table 2. Values in each group were then averaged ("mean of means"). The relative N2BA-titin content in CAD-transplants was 47.0±2.4%—significantly higher ($p<0.05$) than in non-ischemic transplants (32.1±1.4%), CAD donors (29.5±2.6%), and normal donors (28.1±0.8%) (Figure 21). All CAD-transplant hearts showed higher N2BA-titin expression than normal donor hearts. The total amount of titin (N2B+N2BA) was similar in all HH-groups (data not shown). Four non-ischemic transplant hearts were also analyzed and they showed a slight increase in average N2BA percentage compared to donor hearts, 34% ± 4% (Figure 21).

Table 2. Results of gel-electrophoretic titin analysis of individual HHs. Average relative N2BA-titin content (N2BA+N2B=100%) was measured from the optical volume of bands on coomassie-stained 2% SDS gels (n, number of lanes analyzed). Modifications of cTnI were studied on Western blots (10-20% polyacrylamide gradient gels), using TnI-antibody 8I-7. Symbols indicate TnI-band intensity: (-) no; (±) faint; (+) normal; (++) strong band. (from Neagoe et al., 2002).

Heart number	age/ gender	cTnI-degradation/ cTnI-complexes	N2BA-titin (%), mean±SD (n)
CAD Transplants			
HH1	52/M	±/+	53.3±3.5 (18)
HH17	65/M	±/+	48.5±3.6 (7)
HH22	45/M	+/++	39.4±2.3 (6)
HH26	65/F	±/±	49.6±3.1 (5)
HH27	55/F	+/±	44.3±3.7 (7)
Non-ischemic Transplants			
HH3	?/F	-/-	31.2±6.9 (6)
HH4	65/M	±/±	29.1±6.1 (12)
HH12	?/F	-/±	32.6±4.1 (10)
HH21	?/M	+/-	35.7±3.8 (5)
CAD Donors			
HH19	56/M	+/+	37.0±2.3 (7)
HH30	67/F	-/±	25.7±4.6 (6)
HH31	74/M	-/±	28.2±4.3 (6)
HH33	59/M	±/±	27.1±5.6 (4)
Normal Donors			
HH5	51/F	-/-	25.3±3.9 (20)
HH6	43/M	±/±	28.1±2.7 (11)
HH7	16/F	±/±	29.2±3.2 (5)
HH9	56/M	-/-	22.7±4.1 (11)
HH10	64/F	-/-	25.1±3.3 (8)
HH15	23/M	-/-	29.7±3.2 (8)
HH24	67/F	±/-	27.8±1.9 (7)
HH25	54/F	±/+	30.9±3.5 (6)
HH37	?/?	-/-	25.4±3.8 (7)
HH38	?/?	+/-	30.6±3.2 (11)
HH44	?/?	±/-	30.4±2.9 (10)
HH46	?/?	-/-	31.9±4.5 (11)

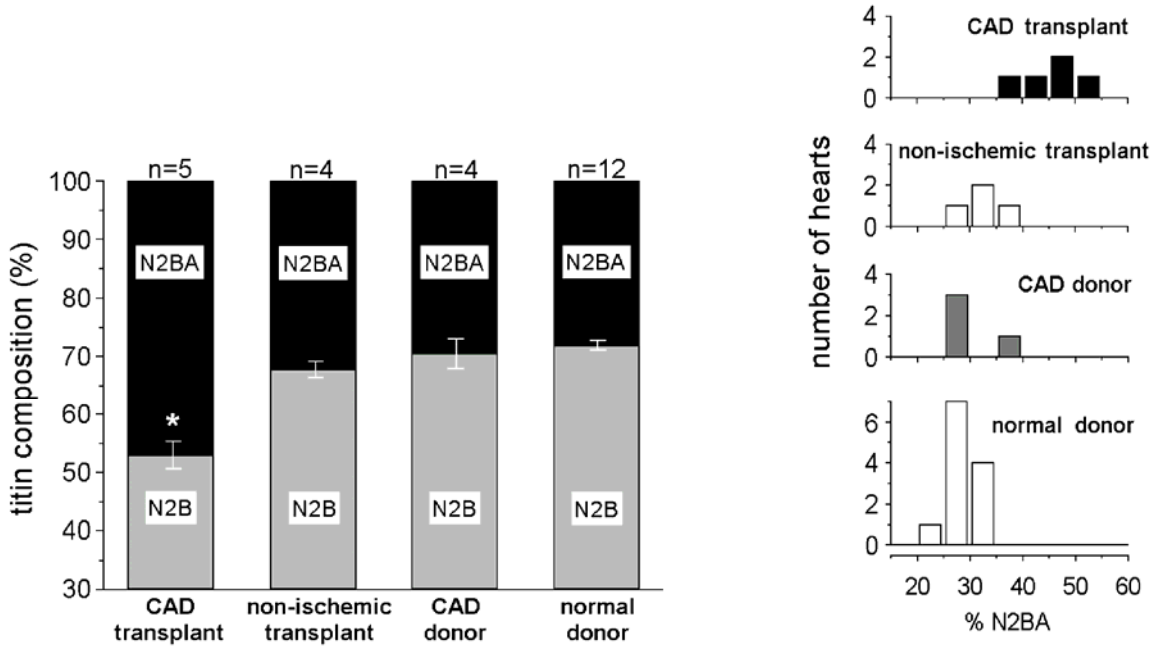

Figure 21. Titin isoform composition in human hearts. Titin band intensities were measured on coomassie-stained 2% SDS-polyacrylamide gels. (Left) Average N2BA + N2B percentage in the four different human heart groups investigated. The CAD transplant group showed more relative N2BA-titin content than any other group (* $p<0.002$ in Student's t-test). (Right) Histogram distribution of N2BA titin (% of N2B + N2BA) in HH groups.

3.2.2 Broadening of the N2BA isoform spectrum in failing myocardium

Not only the N2BA:N2B isoform ratio was assessed in the human hearts, but also the broadness of the titin bands measured on 2% gels by generating an intensity profile and determining the full width at half maximum (FWHM) of the respective peaks (Figure 22). The N2BA band of failing HH samples (LV from dilated cardiomyopathy (DCM) and CAD hearts) was much broader than the N2BA band of normal HHs (Figure 23). In contrast, the N2B-titin band was of similar sharpness in all HH groups. Further, the distance between the centers of mass of the N2B and N2BA peaks was increased in the failing myocardium, demonstrating the increased expression of larger N2BA isoforms. Simulating the intensity profiles as Gaussian distributions again suggested that the N2BA titin is the sum of two closely spaced bands, as the intensity profile could be best fitted by two Gaussian curves (see Figure 18). Thus, human myocardium contains at least two distinct species of N2BA isoform. However, owing to the estimated resolution limit of ~80 kDa in the titin size range, it cannot be excluded that HH expresses a multitude of N2BA-titin isoforms.

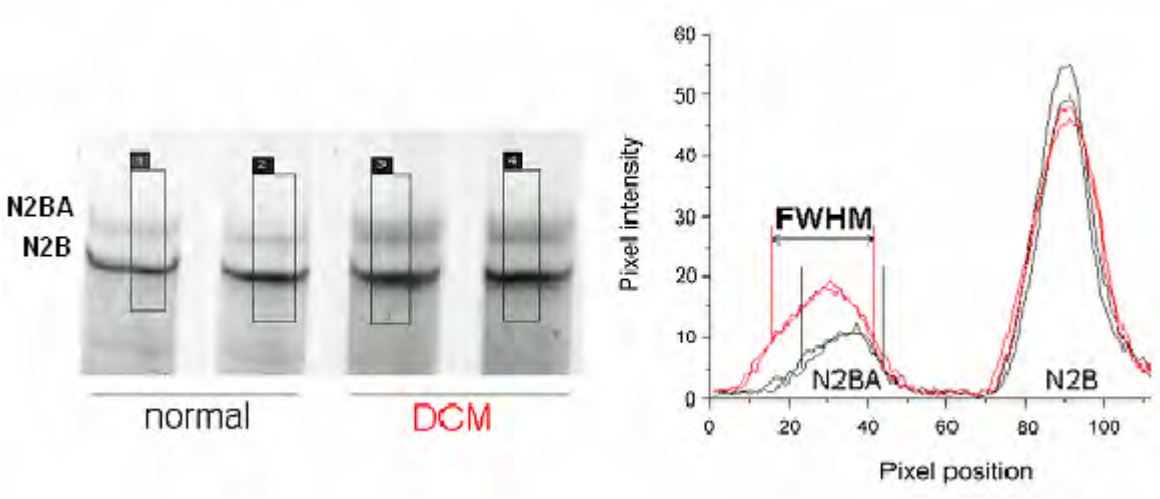

Figure 22. Image of a 2% gel discerning titin isoforms. The N2BA– titin band is broader for the failing heart (here DCM) samples and is shifted towards higher molecular weights. (Right) Intensity profiles (8-bit greyscale) of normal HH and DCM HH lanes.

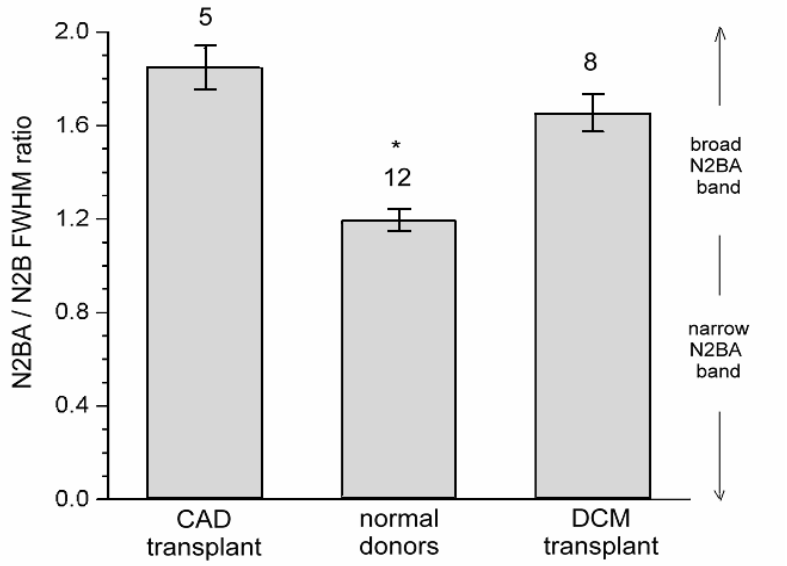

Figure 23. Summary of the titin band FWHM signals. The number of HHs analyzed per group is indicated above the columns. The sharpness of the N2B band was unchanged (for extensive analysis see Makarenko et al., 2004), but the N2BA band was significantly narrower in normal donor than in failing HH samples ($p<0.05$).

3.3 Troponin I analysis

A characteristic that discriminated CAD from DCM or normal donor HHs samples was the presence of ischemia. Even if necrosis is of limited extent in MI, cardiomyopathic processes can nevertheless impair the contractility of the non-infarcted cardiac tissue. A good biomarker for an acute ischemic event (in conjunction with reperfusion injury) was suggested to be the elevated serum concentration of cardiac TnI. Moreover, cTnI was proposed to be a potential predictor of increased risk for progressive ventricular dysfunction and congestive heart failure (Horwich et al., 2003). In the stunned myocardium cTnI undergoes typical modifications, as shown when ischemia was induced in excised rat hearts (McDonough et al., 1999). Interestingly, also increased preload can lead to cTnI degradation (Feng et al., 2001). In this context, I tested whether ischemia produced cTnI modification in non-necrotic regions of CAD HH and whether this was related to changes in titin isoform ratio.

Cardiac TnI modification was assessed by Western blotting (Figure 24). cTnI degradation as well as formation of complexes containing cTnI were detectable when normal HH sample was purposely left to degrade for 1 h at 25°C in the absence of protease inhibitor, leupeptin. Similar alterations to cTnI were seen in CAD HH. Table 2 summarizes the types of cTnI modification seen. In CAD cTnI was more strongly modified than in normal donor HH. These changes appeared to correlate with the degree of changes in titin isoform expression.

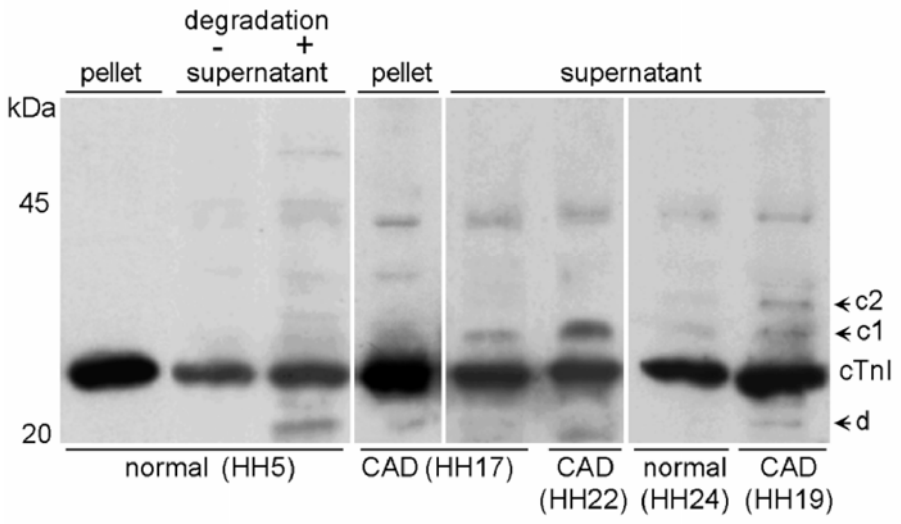

Figure 24. Cardiac troponin I modifications assessed by Western blot (8I-7 antibody). (first two lanes) A normal cardiac (HH5) sample degraded for 1h in absence of leupeptin revealed cross-linking (c) and proteolysis of cTnI (d). (Other lanes) Compared to normal HH, CAD HHs showed substantial cTnI modification. The modified cTnI was similarly present in the "pellet" and "supernatant" fractions, but only the "supernatant" data are reported.

3.4 Structural changes to the myocardium - in situ detection of titin, collagen and desmin

Mechanical overloading often leads to cardiac remodelling, among others affecting the connective tissue, e.g., increasing the collagen content. It was therefore of interest to study in sections of HH tissue (CAD versus donor) the expression of titin along with possible changes in collagen expression. A change in titin isoform pattern could potentially be caused by one or a combination of the following:

a) A loss of titin affecting preferentially the stiff titin isoform, N2B;

b) Upregulation of total titin favouring the N2BA isoform;

c) A true switch of isoforms, where N2BA partially replaces the N2B.

Further, titin changes could occur uniformly in large areas of the heart or affect only some cells or myofibrils and leave others unaffected. To test for this possibility, paraformaldehyde-fixed tissue sections were incubated with titin antibodies of known epitope specificity (also see Freiburg et al., 2000). Fluorescence microscopy showed a regular striated pattern using an antibody directed against the N2A-domain (MG1), with the fluorescence intensity being similar in diseased (CAD) and control (donor) HH samples (Figure 25 A). Similarly, with antibodies to both titin isoforms (N2B and BD6), the staining was comparable between diseased and control tissue (see Neagoe et al., 2002, Figures 4B and 4C).

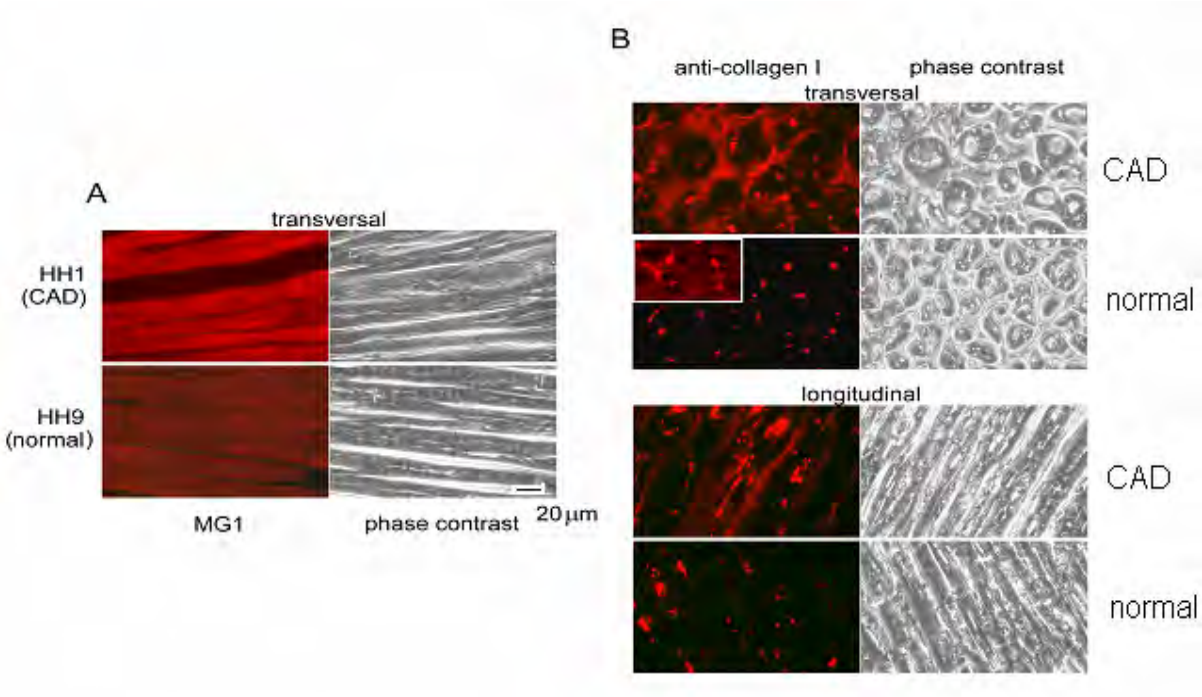

Figure 25. Immunofluorescence microscopy on cardiac muscle sections. (A) Titin staining is regular in normal and CAD samples. (B) Collagen-1 staining around cells is stronger in CAD than in normal HH. Inset: collagen signals after 6x increased primary antibody concentration.

Expression of collagen type I was upregulated in CAD, whereas in normal donor heart collagen staining was generally of low intensity (Figure 25 B). Thus, in CAD hearts the total amount of titin seemed unchanged and the titin isoform switch towards N2BA likely occurred uniformly in large groups of myocytes. In no case could one observe in the diseased myocardium irregularities of the myofibrillar staining for titin. Enlarged extracellular space and misalignment of the fibers were more often found in samples from failing myocardium.

The intermediate filament protein, desmin, also has a mechanical function in cardiac myocytes, as it interconnects parallel sarcomeres at the Z-discs. The myofibrillar localization of desmin was assessed on normal and CAD samples by immunofluorescence microscopy. Desmin was present at the Z-discs and absent in the A-bands or I-bands of the sarcomeres, but its distribution was unchanged in CAD versus donor samples. However, the fluorescence intensity was clearly increased in CAD myofibrils, indicating upregulation of desmin expression (Neagoe et al., 2002).

3.5. Mechanical characteristics of human heart myofibrils

3.5.1 Structural preservation of myofibrils isolated from frozen human heart tissue

Titin and collagen are the two major contributors to passive stiffness in myocardium. The stiffness of the non-activated sarcomeres is generated essentially by titin (Linke et al. 1994), whereas collagen is principally responsible for the stiffness of the extracellular matrix. To test for functional consequences of altered titin isoform expression, isolated myofibrils were prepared from frozen HH tissue, with the aim to measure their passive stiffness. As this was the first time that single myofibrils from frozen human heart were used for mechanical analysis, a number of control experiments were performed to test for the structural preservation of the specimens. Titin was stained using antibodies to the N2A-domain (MG1) and the epitope spacing was measured in stretched HH myofibrils (Figure 26). The epitope spacing across the Z-disc increased with SL, proving the integrity of titin anchorage at the Z-disc and the thick filament. The distance from the epitope to the Z-line at a given SL was not distinguishable between diseased and normal HH myofibrils, and it was comparable with published data obtained for rabbit cardiac myofibrils (Linke et al., 1999).

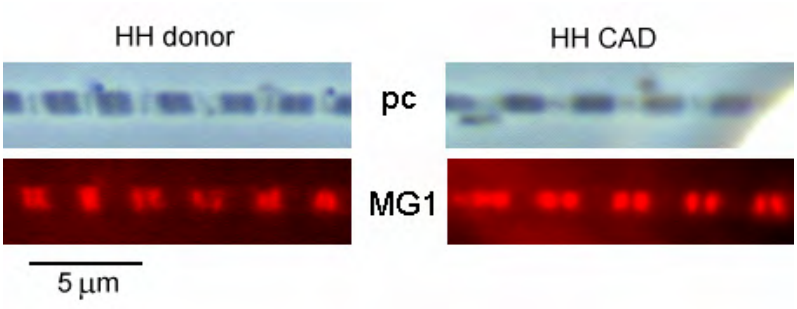

Figure 26. Assessment of the MG1 epitope displacement by stretch demonstrated that in specimens from frozen tissue titin is anchored in the Z-disk and attached to the thick filament.

Another control was to test whether myofibrillar passive stiffness can principally be influenced by sample storage at –80°C. Passive stiffness was therefore measured in myofibrils from frozen or freshly dissected rat LV. No significant difference was noted (data not shown) and it was thus concluded that deep-freezing does not alter the passive mechanical properties of the myofibrils.

3.5.2 Myofibrillar passive stiffness: correlation to N2BA-titin proportion

Force measurements were done to estimate the passive length-tension curves of nonactivated HH myofibrils. Cardiac myofibrils with elevated N2BA-titin content were isolated from HH1 and HH17 (CAD group) as well as HH2 and HH8 (DCM group). Normal myofibrils were obtained from HH6 and HH10. All myofibrils presented a regular sarcomeric pattern and their slack SL was close to 1.85 µm.

Myofibrils of diseased hearts responded to stretch with lower forces than normal HH myofibrils (Figure 27). Differences between passive tension generated by normal myofibrils and CAD myofibrils were significant ($p<0.05$, Student's t-test) at SLs equal to or longer than 2.1 µm. These mechanical changes correlated well with the increased proportions of compliant N2BA titin isoform in CAD samples. Although the CAD myofibrils showed reduced passive stiffness, the CAD hearts were globally stiffened, as judged by the increased LV end-diastolic pressure (LVEDP) (Figure 28). These results suggest that titin-based stiffness is decreased in CAD hearts due to titin-isoform switch, but these changes are more than compensated for by increased collagen stiffness.

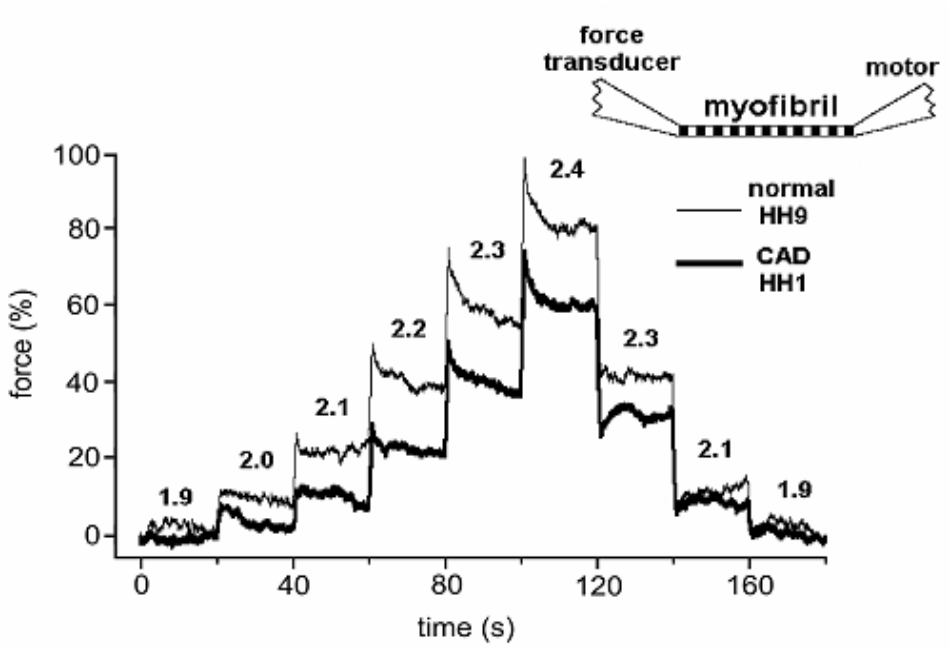

Figure 27. Force measurements on isolated myofibrils from normal and CAD-transplant HH. The specimen was stretched stepwise (SL indicated on top of the force traces), then released to the initial length.

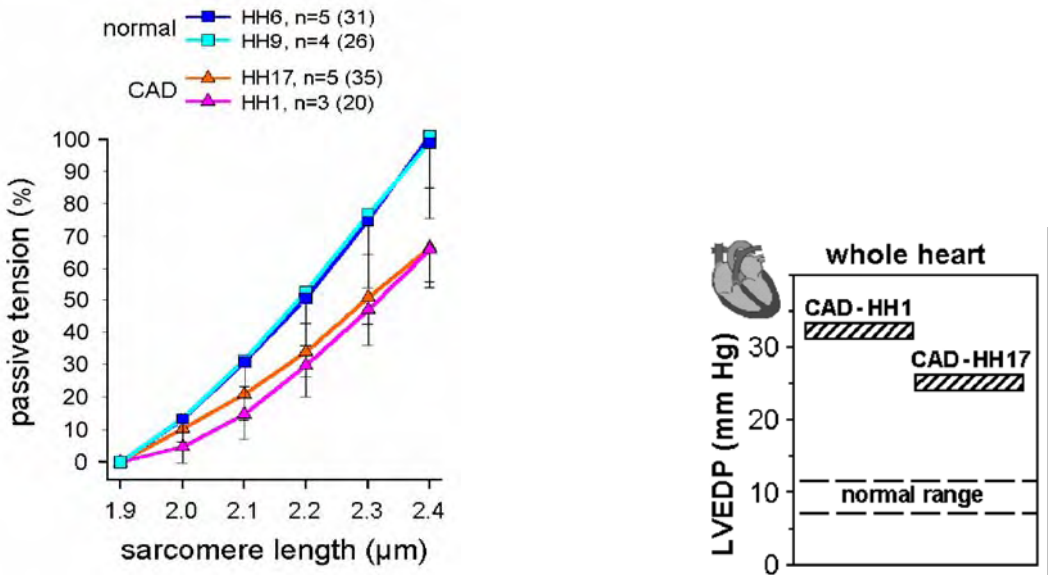

Figure 28. Passive stiffness comparison of CAD versus donor HH samples. (Left) Average quasi-steady-state passive tension at different SLs (100% is the average force at SL = 2.4 μm) for normal and CAD-transplant HH myofibrils. In the interval from 2.1 to 2.4 μm SL, the differences between normal and CAD myofibrils are statistically significant. n, number of myofibrils stretched. (Right) Whole hearts of CAD-transplant showed increased LVEDP compared with the normal range of LVEDP in healthy hearts.

3.6 Titin isoform switching in an experimental model of infarcted rat heart

To test whether ischemic conditions result in a titin isoform shift in an experimental model of heart failure, RV tissue from rats with a ligation of the left anterior descending coronary artery (LAD) (Daniels et al., 2001) were examined for expression of cardiac titin. Non-necrotic tissue was probed for titin on silver-stained titin gels (Figure 29). In all samples a strong N2B titin band was detectable, but in LAD samples there was an increased frequency of an N2BA isoform band appearing above the N2B band. Immunoblot analysis confirmed the identity of the detected titin bands as N2BA and N2B (Figure 29). In LAD rat RV a double titin band was observed in 43% of all samples, in control (sham-operated) RV only in 14%. Results were similar in RVs 12 and 24 weeks after surgery.

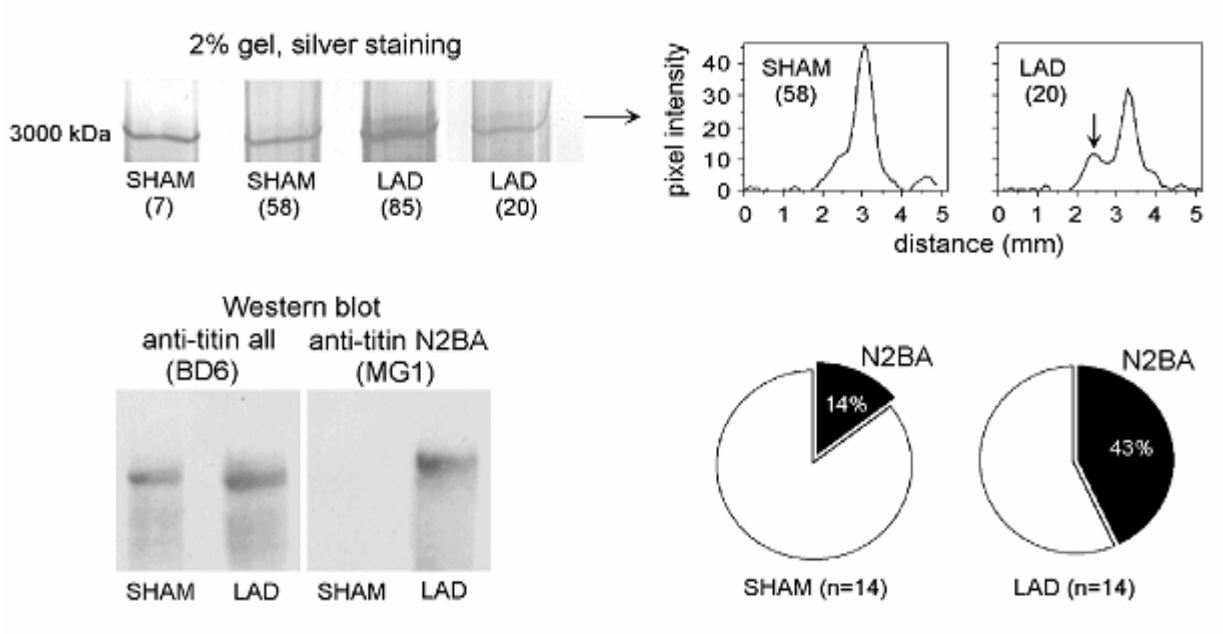

Figure 29. Detection of N2BA-titin in rat myocardium. An N2BA-band sometimes appeared as a distinct peak in the intensity profile plot at the position of N2BA-titin MW. The identity of those bands was determined by Western blot. The frequency of the N2BA band appearance was higher in LAD rat hearts than in sham-operated hearts.

To determine whether the total amount of titin is changed or whether one titin isoform is partially replaced by another, the titin (N2B+N2BA) to MHC ratios were determined in the rat samples. Although the LAD hearts showed significant LV hypertrophy, no alterations in

titin:MHC ratio were detected (Figure 30), suggesting the total titin remained unchanged. However, titin content decreased with age in both LAD and SHAM hearts (Figure 30).

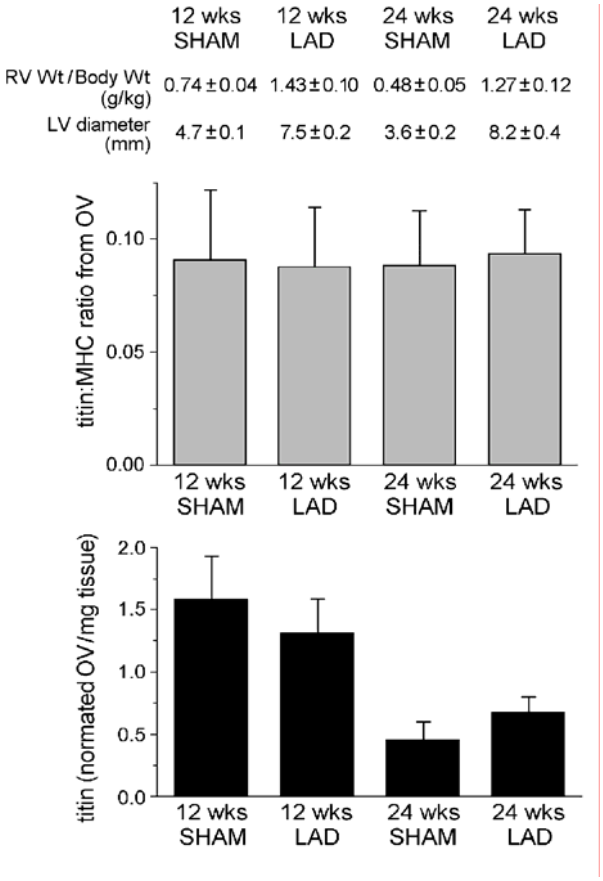

Figure 30. Titin protein content in rat cardiac right ventricle. (Top diagram) 2.8% SDS-PAGE revealed similar titin-to-MHC ratios in LAD and sham-operated specimens (n=8 per column). (Bottom diagram) On silver-stained 2% SDS gels, total cardiac titin content was decreased with age in a statistically significant manner (p<0.05 in Student's t-test) but was similar in LAD and sham-operated animals both 12 and 24 weeks after surgery (n=8 per column). Numbers above diagrams indicate cardiac hypertrophy in LAD (Wt, weight).

3.7 Contribution of the elastic energy to the active contraction of sarcomeres

Recently it was demonstrated that titin conserves the stretch energy in a sarcomere and releases part of it to support muscle contraction (Minajeva et al., 2002). Previous work

suggested that the unloaded shortening velocity of a skeletal muscle increases once the muscle length exceeds a certain value (Edman, 1979). Minajeva et al (2002) showed that the passive recoil of titin in myofibrils is fast, initially reaching velocities an order of magnitude higher than the maximum active shortening speed. Titin's contribution to shortening of rabbit psoas sarcomeres was estimated to be 10% of the contribution from active elements, if the precedent stretch was below 0.7 μm per sarcomere. Up to these stretch amplitudes, the maximum unloaded shortening velocity was nearly constant (Figure 31). At higher sarcomere stretches and therefore higher passive tension, the maximum unloaded shortening velocity of fully activated psoas fibers was significantly increased (Figure 31), likely owing to the contribution of titin elastic recoil to the shortening speed.

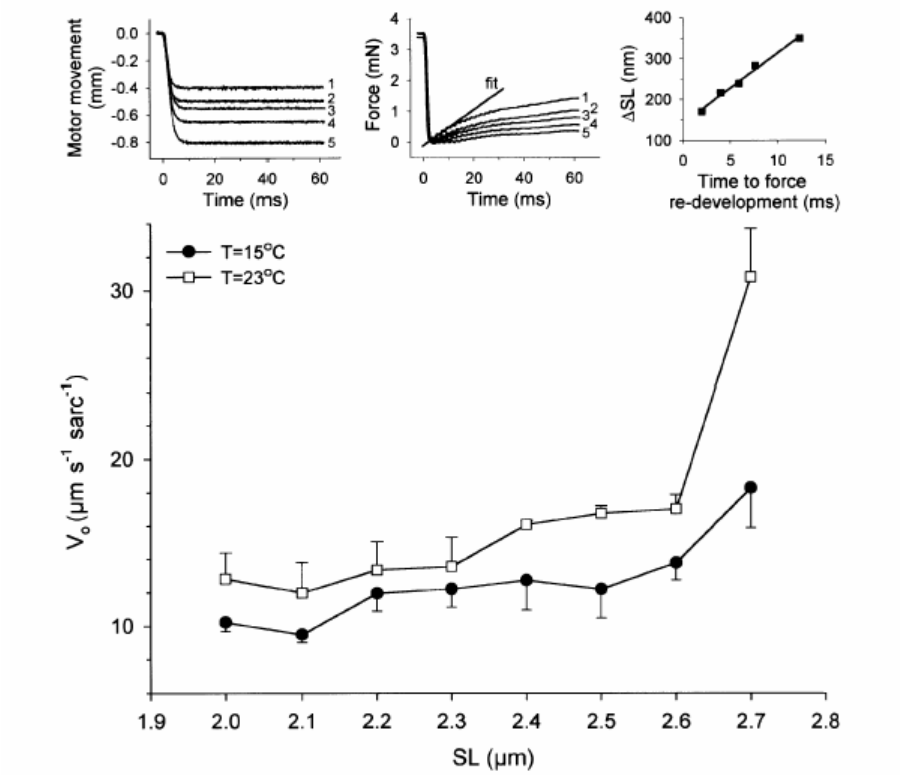

Figure 31. Maximum unloaded shortening velocity of sarcomeres (V_0) in fully activated (pCa 4.5) skinned rabbit psoas fibers. A "slack test" was performed according to Edman (1979). V_0 was constant over a large range of SL, but at high stretch it increased steeply (from Minajeva et al., 2002).

4. DISCUSSION

4.1 Cardiac and skeletal muscle titins can be detected on low porosity SDS-PAGE gels

Titin is encoded by a single gene containing 363 exons in humans. Owing to alternative splicing two major cardiac isoforms are generated, the shorter and stiffer N2B and the longer, more compliant N2BA (Freiburg et al. 2000). Skeletal muscles express the N2A titin isoforms in a muscle-specific manner (Prado et al., 2005). Alteration in titin isoform expression in cardiac muscle leads to a modulation of the titin-based passive tension in chronically diseased hearts (Neagoe et al., 2002). Recently it was demonstrated that cardiac N2BA titin is expressed in various fetal and neonatal isoforms which later disappear in the adult organism, being largely replaced by the N2B isoform (Opitz et al., 2004; Lahmers et al., 2004). How the translation of a giant protein like titin is accomplished in muscle cells is still unknown but it likely requires a precise regulatory machinery perhaps promoting co-translation of titin along with major titin-associated proteins like muscle myosin or alpha-actinin. Titin may be a template for proper muscle assembly and therefore required for normal muscle function.

The initial interest in titin came from its postulated contribution to the passive elasticity of striated muscle. Although several titin isoforms were known to exist in human and other mammalian heart muscles, routine isoform analysis was hampered by the giant size of this protein, which required very loose gels to be prepared. This thesis was aimed at detecting titin isoforms on high resolution 2% SDS-PAGE titin gels, an approach that had not been attempted previously for human heart samples. I found that titin isoforms can indeed be visualized by gel electrophoresis as multiple bands in the megadalton range. Some of these bands corresponding to the intact, full-length, titin molecule were named T1- titin bands, whereas proteolytic degradation products also appearing on the gels were named T2 and T3 titin bands. I observed that titin degradation products, when they exist, are clearly distinguishable on the gels from the intact titin bands (Figure 14) and that modest degradation does not significantly affect the T1 cardiac isoform ratio; the isoforms are equally degraded. This analysis was important, as it allowed a major conclusion to be drawn from my results: the observed titin isoform switch in diseased human hearts is unrelated to titin degradation. This work led up to the first publication on titin isoform analysis in normal and failing (CAD)

human heart (Neagoe et al., 2002), advancing earlier work on cardiac titin expression in other mammalian species (Trombitas et al., 2001; Wu et al 2002).

Another in-depth report on cardiac titin isoform composition and related functional aspects was published later (Makarenko et al., 2004), focusing on human DCM (non-ischemic) heart. Evidence provided by 2% SDS-PAGE demonstrated that failing DCM hearts displayed an asymmetric broadening of the N2BA band compared with normal donor HH, indicating a true shift towards increased expression levels of very high-molecular weight N2BA titin isoforms. Similar findings for DCM samples were reported by Nagueh et al. (2004). These authors also showed a correlation between the extent of the N2BA:N2B titin switch and the severity of the DCM disease state. Yet another study on titin expression in a larger collection of different vertebrate species showed a great variety of titin isoform patterns in different cardiac and skeletal muscles (Neagoe et al., 2003). This work was followed by a study on cardiac titin isoforms in perinatal rat heart development (Opitz et al., 2004), which established the presence of at least four distinct cardiac N2BA-titin isoforms in the course of late embryonic and early postnatal development. The molecular mass of these titins switched from 3700 kDa (N2BA-1) to 3500-3600 kDa (N2BA-2) in the fetus and newborn to 3200 (N2BA-3) and 3400 kDa (N2BA-4) in the adult, the latter isoforms being co-expressed with the predominant N2B titin (3000 kDa). Importantly, in the above experiments the titin:MHC remained unaltered suggesting that the total titin in a sarcomeres may be a rather constant value. This is consistent with models of myofibrillar architecture that do not support a variable stoichiometry between titin and myosin (Liversage et al., 2001).

What could be the reason for the presence of multiple titin isoforms in different muscles or even in the same myofibril and the dramatic isoform switching in development and heart disease? Presumably, the expression of different length titin isoforms in different muscle tissues is a way to adapt passive tension to particular functional (mechanical) needs (Wang et al., 1991). In this context it may be relevant that myocardium expresses N2BA:N2B ratios that show some correlation to the body and heart size of the respective species (Cazorla et al., 2000; Neagoe et al., 2003; Granzier and Labeit, 2002). Why would the hearts of small animals preferentially express the stiff N2B-titin? One can imagine that a mechanical oscillator that has a stiff spring has a higher resonant frequency. For instance, Drosophila indirect flight muscles (IFM) expresses a titin homologue named kettin, which is a comparably short and stiff elastic protein (Kulke et al. 2001 a). Kettin's high stiffness is

necessary for the high frequency working regime of the IFM that drives the wingbeat. Similarly, the low cardiac N2BA:N2B titin isoform ratio in small mammals like rat, mouse or hamster, compared to large mammals like cow, pig or goat, will cause the myofibrils in heart to be relatively stiffer in the former than in the latter. This may be beneficial as the small rodents have a higher heart rate than the large mammals. The higher the heart rate, the greater may be the mechanical stability of the ventricular walls required. However, titin is only one factor contributing to passive stiffness in diastole, as other factors also play a role, such as chamber geometry, ventricular wall thickness, and extracellular matrix proteins (collagen). Nevertheless, titin isoform composition and titin stiffness may be critically important.

It was also proposed that regional differences in titin expression pattern in heart, particularly transmural differences in N2BA:N2B titin ratio, are disturbed under disease conditions, as e.g. follow from chronic pacing (Bell et al. 2000). I analyzed the transmural distribution of the N2BA:N2B ratio but did not detect differences in normal goat heart (Figure 19), non-failing human donor heart (Figure 20), and also in normal sheep, pig and cow heart (data not shown). If they existed at all, transmural differences in titin composition may indeed be small in normal heart, but may be exaggerated in diseased heart (Bell et al., 2000; Wu et al., 2002). In Neagoe et al. (2003) I showed instead that normal heart expresses quite different N2BA:N2B ratios in the different cardiac chambers, as well as at the base compared to the heart's apex.

The signaling pathways causing the titin isoform switch have only very recently been investigated. A recent paper (Krüger et al. 2008) described experiments on developing rat cardiomyocytes in culture exhibiting a titin switch similar to that in rat heart tissue in vivo. It was found that a main trigger for the titin switching is an activation of the phosphoinositol-3-kinase (PI3K) and Akt (protein kinase B) pathways, e.g. by thyroid hormone, triiodo-L-thyronine (T3). Whether deactivation of the PI3K/Akt pathway accounts for the reverse titin isoform switching in human heart disease remains to be shown.

4.2 Collagen and titin: interplay between matrix and myocyte passive stiffness

Chronically diseased human CAD hearts expressed higher relative amounts of compliant N2BA-titin causing decreased myofibrillar passive stiffness (Neagoe et al., 2002). The total concentration of titin (titin:MHC ratio) was not different in diseased and normal

hearts. The titin isoform switch was really a switch of titin in myofibrils, as two different solubilization procedures, a whole tissue homogenate solubilization and a myofibrillar fraction solubilization resulted in the same titin isoform ratio for a given HH sample (data not shown). Initially it was surprising (or at least counter-intuitive) that the titin changes were in the opposite direction of what was expected from the observed global stiffening of the CAD hearts (increased LVEDP; although this does not necessarily mean higher myocardial stiffness). It was therefore speculated that the switch towards increased N2BA titin in failing myocardium is compensatory. As the titin-isoform switching was not the cause of the global stiffening in failing hearts, efforts were undertaken to investigate other determinants of passive stiffness, particularly the intermediate filament protein, desmin, and the collagen (I and III) expression levels. Collagen forms a stiff filamentous network around the muscle cells which limits the extensibility of the heart tissue (Weber, 1997). As for desmin, it was found that expression of this protein in heart is higher in cardiomyopathy than under normal conditions (see Hein et al., 2000, for a review). I could confirm by immunofluorescence microscopy that more desmin is present in the Z-disc of CAD myofibrils. Desmin contributes somewhat to myocyte passive stiffness and elevated desmin may be expected to increase the lateral stiffness and/or resistance to shear stress. However, isolated myofibrils from CAD hearts showed reduced passive stiffness despite upregulation of desmin. Expression changes of desmin could thus not explain the mechanical alterations.

In contrast, collagen I was upregulated in CAD heart tissue and likely accounted for the increased global stiffness. Hence, a working hypothesis was proposed by Neagoe et al. (2002) suggesting that the titin changes towards compliant N2BA isoform may occur in response to the chronically increased extracellular matrix stiffness, compensating the latter to some degree: increased collagen elevates passive stiffness, whereas increased compliant titin lowers it. Whether the titin changes are a cause or rather a consequence of the remodelling in heart failure remains to be established. Clear is that an interplay between collagen and titin is important to tune myocardial passive stiffness.

The titin isoform switch may occur over a relatively long time period, although the titin turnover (at least in developing heart) can be rather rapid, a few days (Opitz et al., 2004). In a rat model of myocardial infarction (LAD ligature) the number of LAD hearts showing upregulated N2BA titin was not much different 12 weeks following LAD surgery than 24 weeks following surgery. In general the titin changes seen in the rat model were mild

compared those seen in human heart failure. This finding could be related to the fact that the LAD model does not closely mimic the chronic ischemia-induced CAD in humans. Revascularization and natural bypasses around the ligated artery are presumed to compensate the induced dysfunction in rat but such arterial remodelling may not occur in human disease. In any case, the studies on the LAD model of myocardial infarction demonstrated that it is possible to induce a titin isoform shift. However, the time course of the titin isoform switching remains to be established.

4.3 Consequences of titin isoform switching for myocyte mechanical function

Altered passive stiffness. Previous studies on skeletal muscles showed a correlation between titin-isoform size and passive tension at the single-fiber level (Wang et al., 1991; Horowits, 1992; Freiburg et al., 2000) and the single-myofibril level (Linke et al., 1996; Linke, 2000; Kulke et al., 2001 b). Differences in passive tension between cardiac, psoas and soleus myofibrils of rabbit were demonstrated by Neagoe et al. (2003). The two types of skeletal myofibrils studied showed a relatively long initial range of low passive tension, before the curves began to increase more steeply. This was interesting in light of early reports describing two distinct phases of passive-tension development in whole skeletal muscle – a low force, nearly linear phase followed by a highly nonlinear rise in force (Roy, 1881; Haycraft, 1904). Apparently, these passive-tension characteristics can be found also at the level of the single myofibril. Relatively lower passive tension was seen in soleus myofibrils expressing 3700 kDa titin N2A isoform than in psoas myofibrils expressing 3300–3400 kDa N2A titin (Neagoe et al., 2003). Thus, skeletal muscles can achieve lower or higher myofibrillar stiffness by expressing longer or shorter I-band-titin, respectively. The number of titin molecules in a sarcomere (which could also affect stiffness) is unlikely to vary greatly, due to stoichiometric constraints; there is evidence that the number of titin molecules per half thick filament is six (Liversage et al., 2001; Knupp et al., 2002). Compared to skeletal myofibrils, passive tension was much higher at any given SL in myofibrils from rabbit LV (Neagoe et al., 2003) and a somewhat shallower passive SL tension curve was found in myofibrils from human LV. This result correlates well with the differences in N2BA:N2B titin-isoform ratio, ~17:83 in rabbit LV, but ~30:70 in normal human LV (Neagoe et al., 2003). In summary, titin-isoform switching is a way to adjust titin-based myocyte stiffness in both cardiac and skeletal muscle.

Altered restoring forces and A-band centering properties. It was proposed that titin accounts in part for the forces that restore the length of the sarcomere after contraction (shortening) (Helmes et al., 1996). Titin also helps center the A-band in the sarcomere. A stiff titin should generate sufficient restoring forces and reset A-band central location in the sarcomere during diastole (Wu et al., 2000). A switch towards more compliant titin, as seen in heart failure, could compromise these functions of titin. The titin modifications could thus alter diastolic as well as systolic mechanical properties.

Altered active force generation via effects on the Frank-Starling mechanism. Titin was proposed to play a role as a "length sensor" responsible for stretch induced Ca^{2+} sensitization of force, or length-dependent activation (LDA), the molecular basis for the Frank Starling mechanism of the heart (Fukuda et al., 2001; Cazorla et al., 2001). Titin could affect the lateral myofilament spacing by generating a force perpendicular to the myofibrillar axis (Cazorla et al., 2001). A narrower spacing, as seen after sarcomere stretch, would allow myosin crossbridges to interact with actin more efficiently, which would increase the Ca^{2+}-sensitivity. Sarcomeric passive tension levels and calcium sensitivity were indeed correlated and titin was proposed to be important for this effect (Fukuda et al., 2001; Cazorla et al., 2001). Titin isoform shift towards N2BA may affect LDA by lowering the lateral compressive forces and thereby be detrimental for the Frank Starling mechanism.

Altered viscoelasticity via effects on titin's actin-binding properties. Our group and others reported that titin interacts with actin filaments in the PEVK region and that this (weak) interaction generates an internal viscous load (Kulke et al., 2001 b; Yamasaki et al., 2001). Interactions between titin and actin filaments towards the free end of the thin filaments were also suggested to stabilize the sarcomeric architecture (Eremia, 2001). Passive shortening of the stretched sarcomeres arises from titin elastic recoil but viscous damping of the titin recoil probably originates in PEVK-actin interactions (Minajeva et al., 2002). The titin–actin interaction via the PEVK-region is likely to be dependent on titin-isoform expression. The length and the predicted isoelectric point of the PEVK-domain differ much between the N2B and N2BA titins (Greaser et al., 2001; Greaser et al., 2002). Thus, variable PEVK length may be a source of variability in internal viscous loading. Increased viscous drag in myocytes expressing relatively more of the long N2BA isoforms could affect the myofilament sliding speed in failing hearts, thereby reducing contractility.

4.4 TnI modification – a sign of increased preload or chronic ischemia?

For most CAD hearts, the LVEDP was not available. To compensate, an indirect method of assessment was developed based on the assumption that cTnI modifications apparent on Western blots of failing heart tissue could be a marker for the degree of ischemic-reperfusion damage (McDonough et al., 1999). Another report later suggested that cTnI modification may be a sign of chronically increased preload, instead of ischemia (Feng et al., 2001). The latter was reason for us to study cTnI proteolysis and complex formation (cTnI covalently bound to other troponin isoform fragments; McDonough et al. 1999) in the human CAD samples along with the changes in titin isoform composition. Indeed, the CAD transplant samples showed, on average, greater cTnI modifications than normal donor human hearts. Whether these alterations were causally related to changes in titin composition or were merely coincidental could not be assessed. If the increased TnI modification in human heart failure indeed indicated chronically increased preload, the titin changes could be caused by overloading the heart in diastole. This interesting possibility could be investigated in the future, e.g. using cell culture systems where preload and ischemia can be manipulated independently.

4.5 Perspective: Establishing a cell culture model system to study cardiac titin isoforms

Invited by Prof. Dr. Hans Eppenberger from the Institute of Cell Biology at the ETH Zurich (Switzerland), I had the opportunity to examine titin isoform expression in adult rat cardiomyocytes in long term cell culture. These experiments were thought as a first step towards establishing a cell culture model in which one could study the signaling pathways underlying the titin isoform switch in heart development and disease. The cardiac cells were derived from adult rat heart tissue and when cultured long-term, they expressed N2BA and N2B titin isoforms as demonstrated by immunofluorescence microscopy (data not shown). MG1 antibody to the N2A-domain displayed a doublet band around the Z-disc once the sarcomeres were stretched. These experiments paved the way for a systematic, extensive study of titin isoform switching in cultured developing rat cardiomyocytes, which established a central role of the PI3K/Akt signaling pathway for the titin isoform transition (Krüger et al., 2008).

4.6 Conclusions

The main conclusions from this work are as follows:

1) Cardiac muscles express various titin isoforms; the ratio between N2BA titin and N2B titin is species-specific;

2) The ratio between N2BA and N2B titin is ~30:70 in normal human heart, but can increase to nearly 50:50 in hearts from end-stage CAD patients;

3) Widening of the N2BA-titin isoform expression spectra is often found in end-stage CAD and DCM hearts, where longer-than-normal N2BA–titins are expressed;

4) The titin isoform switching in human heart lowers sarcomeric passive stiffness;

5) Although titin-based stiffness is decreased in failing human hearts, these hearts are globally stiffened due to increased fibrosis;

6) The titin modifications might partially counteract the elevated stiffness due to increased collagen expression;

7) Higher than normal or unchanged N2BA:N2B titin ratios may be found under different disease conditions;

8) Further studies are necessary to characterize the signals that determine the disease-related changes in cardiac titin isoform composition.

5. SUMMARY

Background: Titin is a giant elastic protein of muscle sarcomeres. Titin molecules link the Z-disk with the M-line and have structural, elastic and signaling functions in myocytes. The primary structure determination of several titin isoforms and the mechanical characterization of different muscle tissues revealed that titin elasticity depends on the differential splicing of the titin spring region consisting of immunoglobulin-like domains, a so-called PEVK domain and larger unique sequence insertions like N2-B. The molecular weight of a titin isoform is correlated with its mechanical, spring-like properties: the smaller the isoform, the stiffer the spring. Heart muscles of mammalian organisms co-express two major classes of titin isoforms: the stiff N2B-titin and the compliant N2BA-titin. Sarcomeric stiffness is tuned by altering the expression ratio of N2BA:N2B titins, whereas the amount of total titin in a sarcomere likely is constant owing to stoichiometric constraints.

Objectives of the study: 1) To determine the patterns of titin isoform expression in different muscle tissues using MDa-range high-resolution gel electrophoresis and Western blotting; 2) To understand the functional significance of the expression of various cardiac titin isoforms; 3) To look for variations in cardiac titin expression in diseased myocardium; 4) To establish conditions/factors determining different expression patterns of cardiac titin; 5) To understand consequences of pathological changes in titin protein expression for the heart.

Methods and Results: N2BA to N2B titin isoform ratio was determined by loose-gel electrophoresis. The titin isoform ratio differed between: 1) Hearts from different mammalian species; 2) Various regions of the same heart; 3) Diseased and normal human hearts. Western blotting using sequence assigned anti-titin antibodies confirmed the identity of the titin bands. The N2BA proportion varied from ~5% in rat left ventricle to almost 70% in cow right ventricle. The N2BA:N2B ratio was generally higher in the right ventricle than in the corresponding plane of the left ventricle and decreased from the base to the apex of a given heart (assessed in goat and rabbit). Titin isoform expression was altered under disease conditions: human heart transplants due to coronary artery disease (CAD) exhibited an average N2BA:N2B ratio of 47:53, whereas normal donor hearts had a ratio of ~30:70. Increased expression of larger N2BA titin isoforms was also seen in failing myocardium of dilated cardiomyopathy (DCM) patients.

Coexpression of N2BA-titin and N2B-titin in a sarcomere was demonstrated by immunofluorescence microscopy. A regular cross-striated staining pattern for titin on tissue

sections of CAD-transplant hearts indicated uniform changes of titin expression instead of titin structural damage. The functional relevance of the observed changes in titin isoform expression was estimated in mechanical experiments on isolated myofibrils from human hearts. Diseased (CAD, DCM) human myofibrils expressing elevated N2BA proportions had lowered passive stiffness compared to non-failing human myofibrils. Thus, sarcomeres can modify their passive tension by adjusting the N2BA:N2B titin expression ratio. Failing human hearts, even if they are globally stiffened (collagen upregulated), have more compliant myofibrils than normal donor human hearts.

Titin isoform switching was also studied in a rat model of myocardial infarction (ligature of left anterior descending coronary artery). Titin gels showed that 43% of diseased hearts displayed a distinct N2BA-titin band, compared to only 14% of the hearts of sham-operated control rats, suggesting an isoform switch had occurred in this heart failure model.

Conclusions: An improved titin detection method by modified 2% SDS-polyacrylamide gel electrophoresis revealed the presence of multiple titin isoforms in different tissues. Results established that the elastic diversity of titin is altered in human heart disease and during development. The shift towards expression of more compliant titin isoforms in human heart failure alters mechanical properties of the cardiomyocytes, in particular the passive stiffness. The disease-induced shift in titin isoform ratio may also impair active contraction, e.g. by interfering with the ability of the heart to use the Frank-Starling mechanism.

ZUSAMMENFASSUNG

Hintergrund: Titin ist ein riesiges elastisches Protein der Muskelsarkomere. Titin-Moleküle verbinden die Z-Scheibe mit der M-Linie und haben strukturelle, elastische und Signalfunktionen in den Myozyten. Die Primärstrukturermittlung einiger Titinisoformen und die mechanische Charakterisierung verschiedener Muskelgewebe zeigten, dass die Titinelastizität durch differenzielles Spleißen der Titin-Federregion moduliert wird, indem unterschiedlich lange Segmente eingebaut werden bestehend aus Immunglobulin-artigen Domänen, einer so genannten PEVK-Region und größeren einzigartigen Sequenzinsertionen wie N2-B. Das Molekulargewicht einer Titinisoform korreliert mit seinen Federeigenschaften: je kleiner (kürzer) die Isoform, desto steifer die Feder. Die Herzmuskeln von Säugern koexprimieren zwei Haupt-Titinisoformen, das steife N2B-Titin und das weniger steife N2BA-Titin. Die Sarkomer-Steifigkeit wird durch Einstellung des Expressionsverhältnisses von N2BA zu N2B justiert, während die Gesamttitinmenge in einem Sarkomer wohl aufgrund stöchiometrischer Restriktionen konstant ist.

Zielsetzungen der Arbeit: 1) Ermittlung des Titinisoformenexpressionsmusters in verschiedenen Muskelgeweben unter Verwendung von hochauflösender Gelelektrophorese und Western blot; 2) Aufzeigen der funktionalen Bedeutung der Expression verschiedener Herztitinisoformen; 3) Analyse möglicher Veränderungen in der Expression des Herztitins im kranken Myokard; 4) Etablierung von Faktoren, die für das Herz-Titinexpressionsmuster relevant sind; 5) Verstehen der Konsequenzen der pathologischen Änderungen in der Titinexpression für das kranke Herz.

Methoden und Ergebnisse: Das N2BA:N2B Titinisoformenverhältnis wurde durch Elektrophorese unter Verwendung besonders poröser Polyacrylamidgele bestimmt. Das Titinisoformenverhältnis war unterschiedlich: 1) in den Herzen von verschiedenen Säugetier-Species; 2) in verschiedenen Regionen des gleichen Herzens; und 3) in kranken gegenüber normalen menschlichen Herzen. Western Blots unter Verwendung sequenzspezifischer Titinantikörper bestätigten die Identität der Titinbanden. Der N2BA-Anteil schwankte von ~5% im linken Ventrikel der Ratte bis nahezu 70% im rechten Ventrikel der Kuh. Das N2BA:N2B Verhältnis war im Allgemeinen im rechten Ventrikel größer als im linken Ventrikel und war an der Herzbasis leicht höher als an der Herzspitze ein und desselben Herzens (untersucht in Ziege und Kaninchen). Das Titinisoformenmuster war in kranken humanen Herzen verändert: in wegen Koronararterienkrankheit (CAD) transplantierten

Herzen bestand ein durchschnittliches N2BA:N2B Verhältnis von 47:53, während normale Spenderherzen ein Verhältnis von ~30:70 zeigten. Ein erhöhter Expressionsanteil der größeren N2BA-Titinisoform wurde auch in den Herzen von Patienten mit Dilatativer Kardiomyopathie (DCM) beobachtet.

Eine Koexpression von N2BA- und N2B-Titin im gleichen Sarkomer wurde mittels Immunfluoreszenzmikroskopie gezeigt. Ein regelmäßiges quergestreiftes Färbemuster für Titin auf Gewebeabschnitten von CAD-Herzen deutete auf eine uniforme Veränderung der Titinexpression hin, nicht aber auf strukturelle Schäden im Titin. Die funktionale Bedeutung der beobachteten Titinexpressionsveränderungen wurde in mechanischen Experimenten mit isolierten Myofibrillen menschlicher Herzen untersucht. Kranke Myofibrillen (CAD, DCM) mit erhöhtem N2BA-Anteil offenbarten eine abgesenkte passive Steifigkeit im Vergleich mit Myofibrillen aus normalen Donorherzen. Die Sarkomere konnten also ihre passive Spannung ändern, indem sie das N2BA:N2B Expressionsverhältnis modulierten. Insuffiziente humane Herzen haben demzufolge, selbst wenn sie global versteift sind (Kollagen hochreguliert), schlaffere Myofibrillen als normale menschliche Spenderherzen.

Eine Titinisoformenveränderung wurde auch an einem Rattemodell mit experimentellem Myokardinfarkt nach LAD-Ligatur untersucht. Titingele zeigten, dass 43% der kranken Herzen eine eindeutige N2BA-Bande aufwiesen, während nur 14% der Herzen Sham-operierter Tiere eine N2BA-Bande zeigten. Die Befunde demonstrierten, dass in diesem Tiermodell eine Titin-Isoformenveränderung hin zu N2BA induzierbar war.

Schlussfolgerungen: Eine verbesserte Titinisoformendetektion durch Verwendung niedrigprozentiger (2%) SDS-Polyacrylamid-Gele offenbarte das Vorhandensein vieler verschieden großer Titinisoformen in unterschiedlichen Muskelgeweben. Die Arbeit dokumentiert die elastische Vielfalt des Titins sowie deren Veränderungen bei menschlichen Herzerkrankungen und in der Entwicklung. Die Veränderung hin zu schlaffen N2BA-Isoformen im terminal insuffizienten humanen Herzen beeinflusst die mechanischen Eigenschaften der Kardiomyozyten, insbesondere deren passive Steifigkeit. Die krankheitsbedingte Verschiebung im Titinisoformenverhältnis könnte auch die Kontraktilität verschlechtern, indem z.B. die Fähigkeit des Herzens, den Frank-Starling-Mechanismus zu verwenden, behindert wird.

6. REFERENCES

Anderson J, Joumaa V, Stevens L, Neagoe C, Li Z, Mounier Y, Linke WA and Goubel F (2002)

Passive stiffness changes in soleus muscles from desmin knockout mice are not due to titin modifications.

Pflügers Arch. 444: 771-776.

Antohe F, Popov D, Rãdulescu L, Simionescu N, Börchers T, Spener F, Simionescu M. (1998)

Heart microvessels and aortic endothelial cells express 15 kDa heart-type fatty acid binding proteins.

Eur J Cell Biol. 76: 102-109.

Bang ML, Centner T, Fornoff F, Geach AJ, Gotthardt M, McNabb M, Witt CC, Labeit D, Gregorio CC, Granzier H and Labeit S (2001)

The complete gene sequence of titin, expression of an unusual approximately 700-kDa titin isoform, and its interaction with obscurin identify a novel Z-line to I-band linking system.

Circ Res. 89: 1065-1072.

Bell SP, Nyland L, Tischler MD, McNabb M, Granzier H and LeWinter MM (2000)

Alterations in the determinants of diastolic suction during pacing tachycardia.

Circ Res. 87: 235-240.

Bowles NE, Bowles KR, Towbin JA (2000)

The "final common pathway" hypothesis and inherited cardiovascular disease. The role of cytoskeletal proteins in dilated cardiomyopathy.

Herz 25: 168-175.

Carrion-Vazquez M, Oberhauser AF, Fowler SB, Marszalek PE, Broedel SE, Clarke J and Fernandez JM (1999)

Mechanical and chemical unfolding of a single protein: a comparison.

Proc Natl Acad Sci USA 96: 3694-3699.

Cazorla O, Vassort G, Garnier D, Le Guennec JY (1999)

Length modulation of active force in rat cardiac myocytes: is titin the sensor?

J Mol Cell Cardiol. 31: 1215-1227.

Cazorla O, Freiburg A, Helmes M, Centner T, McNabb M, Wu Y, Trombitas K, Labeit S and Granzier H (2000)

Differential expression of cardiac titin isoforms and modulation of cellular stiffness.

Circ Res. 86: 59-67.

Cazorla O, Wu Y, Irving TC and Granzier H (2001)

Titin-based modulation of calcium sensitivity of active tension in mouse skinned cardiac myocytes.

Circ Res. 88: 1028-1035.

Clark KA, McElhinny AS, Beckerle MC and Gregorio CC (2002)

Striated muscle cytoarchitecture: An intricate web of form and function.

Annu Rev Cell Dev Biol. 18: 637-706.

Daniels MC, Keller RS, de Tombe PP (2001)

Losartan prevents contractile dysfunction in rat myocardium after left ventricular myocardial infarction.

Am J Physiol Heart Circ Physiol. 281: H2150-2158.

Edman K A (1979)

The velocity of unloaded shortening and ist relation to sarcomere length and isometric force in vertebrate muscle fibres.

J Physiol. 291: 143–159.

Eppenberger-Eberhardt M, Aigner S, Donath M, Kurer V, Walther P, Zuppinger C, Schaub M, Eppenberger HM (1997)

IGF-I and bFGF differentially influence atrial natriuretic factor and alpha-smooth muscle actin expression in cultured atrial compared to ventricular adult rat cardiomyocytes.

J Mol Cell Cardiol. 29: 2020-2039.

Eremia D. (2001)

An explanation of shortening heat generation and mechanical performance enhancement during muscle stretch.

Scientific World Journal. 1: 547-554.

Evans E, Ritchie K (1999)

Strength of a weak bond connecting flexible polymer chains.

Biophys J. 76: 2439-2447.

Feng J, Schaus BJ, Fallavollita JA, Lee TC, Canty JM Jr (2001)
Preload induces troponin I degradation independently of myocardial ischemia.
Circulation 103: 2035-2037.

Freiburg A, Trombitas K, Hell W, Cazorla O, Fougerousse F, Centner T, Kolmerer B, Witt C, Beckmann JS, Gregorio CC, Granzier H and Labeit S (2000)
Series of exon-skipping events in the elastic spring region of titin as the structural basis for myofibrillar elastic diversity.
Circ Res. 86: 1114-1121.

Fukuda N, Sasaki D, Ishiwata S and Kurihara S (2001)
Length dependence of tension generation in rat skinned cardiac muscle: role of titin in the Frank-Starling mechanism of the heart.
Circulation 104: 1639-1645.

Funatsu T, Higuchi H and Ishiwata S (1990)
Elastic filaments in skeletal muscle revealed by selective removal of thin filaments with plasma gelsolin.
J Cell Biol. 110: 53-62.

Fürst DO, Osborn M, Nave R and Weber K (1988)
The organization of titin filaments in the half-sarcomere revealed by monoclonal antibodies in immunoelectron microscopy: a map of ten nonrepetitive epitopes starting at the Z line extends close to the M line.
J Cell Biol. 106: 1563-1572.

Fürst DO, Nave R, Osborn M, Weber K (1989)
Repetitive titin epitopes with a 42 nm spacing coincide in relative position with known A band striations also identified by major myosin-associated proteins. An immunoelectron-microscopical study on myofibrils.
J Cell Sci. 94: 119-125.

Gautel M and Goulding D (1996)
A molecular map of titin/connectin elasticity reveals two different mechanisms acting in series.
FEBS Lett 385: 11-14.

Gautel M. (1996)
The super-repeats of titin/connectin and their interactions: glimpses at sarcomeric assembly.
Adv. Biophys. 33: 27-37.

Gerull B, Gramlich M, Atherton J, McNabb M, Trombitas K, Sassae Klaasen S, et al. (2002)
Mutations of TTN, encoding the giant muscle filament titin, cause familial dilated cardiomyopathy.
Nature Genet. 30: 201-204.

Granzier HL and Irving TC (1995)
Passive tension in cardiac muscle: contribution of collagen, titin, microtubules, and intermediate filaments.
Biophys J. 68: 1027-1044.

Granzier H, Kellermayer M, Helmes M and Trombitas K (1997)
Titin elasticity and mechanism of passive force development in rat cardiac myocytes probed by thin-filament extraction.
Biophys J. 73: 2043-2053.

Granzier H and Labeit S (2002)
Cardiac titin: an adjustable multi-functional spring.
J Physiol. 541: 335-342.

Greaser M (2001)
Identification of new repeating motifs in titin.
Proteins 43: 145–149.

Greaser M, Berri M, Warren CM, Mozdziak PE (2002)
Species variations in cDNA sequence and exon splicing patterns in the extensible I-band region of cardiac titin: relation to passive tension.
J Muscle Res Cell Motil. 23: 473–482.

Gregorio CC, Granzier H, Sorimachi H and Labeit S (1999)
Muscle assembly: a titanic achievement?
Curr Opin Cell Biol. 11: 18–25.

Haycraft JB (1904)
The elasticity of animal tissues.
J Physiol. 31:392-409

Head JG, Houmeida A, Knight PJ, Clarke AR, Trinick J, and Brady RL (2001)
Stability and folding rates of domains spanning the large A-band super-repeat of titin.
Biophys J. 81: 1570-1579.

Hein S, Scholz D, Fujitani N, Rennollet H, Brand T, Friedl A, Schaper J. (1994)
Altered expression of titin and contractile proteins in failing human myocardium.
J Mol Cell Cardiol. 26: 1291-1306.

Hein S, Kostin S, Heling A, Maeno Y, Schaper J (2000)
The role of the cytoskeleton in heart failure.
Cardiovasc Res. 45: 273-278.

Helmes M, Trombitás K, Granzier H. (1996)
Titin develops restoring force in rat cardiac myocytes.
Circ Res. 79: 619-626.

Helmes M, Trombitás K, Centner T, Kellermayer M, Labeit S, Linke WA and Granzier H (1999)
Mechanically driven contour-length adjustment in rat cardiac titin's unique N2B sequence: Titin is an adjustable spring.
Circ Res. 84: 1339-1352.

Horowits R (1992) Passive force generation and titin isoforms in mammalian skeletal muscle.
Biophys J. 61: 392–398.

Horwich TB, Patel J, MacLellan WR, Fonarow GC (2003)
Cardiac troponin I is associated with impaired hemodynamics, progressive left ventricular dysfunction, and increased mortality rates in advanced heart failure.
Circulation. 108: 833-838.

Hunter RJ, Neagoe C, Jarvelainen HA, Martin CR, Lindros KO, Linke WA, Preedy VR (2003).
Alcohol affects the skeletal muscle proteins, titin and nebulin in male and female rats.
J Nutr. 133: 1154-1157.

Huxley HE and Hanson J (1954).
Changes in the cross-striations of muscle during contraction and stretch and their structural interpretation.
Nature, Lond., 173: 149-152.

Huxley AF and Niedergerke R. (1954).
Interference microscopy of living muscle fibres.
Nature, Lond., 173: 971-973.

Isenberg G and Klöckner U (1982).
Calcium tolerant ventricular myocytes prepared by preincubation in a "KB medium".
Pflugers Arch. 395: 6-18.

Itoh Y, Suzuki T, Kimura S, Ohashi K, Higuchi H, Sawada H, Shimizu T, Shibata M and Maruyama K (1988)
Extensible and less-extensible domains of connectin filaments in stretched vertebrate

skeletal muscle sarcomeres as detected by immunofluorescence and immunoelectron microscopy using monoclonal antibodies.
J Biochem. 104: 504-508.

Kellermayer MS, Smith SB, Granzier HL and Bustamante C (1997)
Folding-unfolding transitions in single titin molecules characterized with laser tweezers.
Science 276: 1112-1116.

Kellermayer MS, Smith SB, Bustamante C and Granzier HL (2001)
Mechanical fatigue in repetitively stretched single molecules of titin.
Biophys J. 80: 852-863.

Knupp C, Luther PK and Squire JM (2002)
Titin organisation and the 3D architecture of the vertebrate-striated muscle I-band.
J Mol Biol. 322: 731–739.

Krüger M, Sachse C, Zimmermann WH, Eschenhagen T, Klede S, Linke WA (2008)
Thyroid hormone regulates developmental titin isoform transitions via the phosphatidylinositol-3-kinase/ AKT pathway.
Circ Res. 102: 439-447.

Kulke M, Neagoe C, Kolmerer B, Minajeva A, Hinssen H, Bullard B and Linke WA (2001 a)
Kettin, a major source of myofibrillar stiffness in *Drosophila* indirect flight muscle.
J Cell Biol. 154: 1045-1057.

Kulke M, Fujita-Becker S, Rostkova E, Neagoe C, Labeit D, Manstein DJ, Gautel M and Linke WA (2001 b)
Interaction between PEVK-titin and actin filaments: origin of a viscous force component in cardiac myofibrils.
Circ Res. 89: 874-881.

Labeit S, Barlow D, Gautel M, Gibson T, Holt J, Hsieh C-L, Francke U, Leonard K, Wardale J, Whiting A and Trinick J (1990)
A regular pattern of two types of 100-residue motif in the sequence of titin.
Nature 345: 273-276.

Labeit S and Kolmerer B (1995)
Titins, giant proteins in charge of muscle ultrastructure and elasticity.
Science 270: 293-296.

Laemmli UK (1970)
Cleavage of structural proteins during the assembly of the head of bacteriophage T4.
Nature 227: 680-685.

Lahmers S, Wu Y, Call DR, Labeit S, Granzier H (2004)
Developmental control of titin isoform expression and passive stiffness in fetal and neonatal myocardium.
Circ Res. 94: 505–513.

Leahy DJ, Hendrickson WA, Aukhil I, Erickson HP (1992)
Structure of a fibronectin type III domain from tenascin phased by MAD analysis of the selenomethionyl protein.
Science. 258: 987-991.

Leake MC, Wilson D, Bullard B, Simmons RM (2003)
The elasticity of single kettin molecules using a two-bead laser-tweezers assay.
FEBS Lett. 535: 55-60.

Leake MC, Wilson D, Gautel M, Simmons RM (2004)
The elasticity of single titin molecules using a two-bead optical tweezers assay.
Biophys J. 87: 1112-1135.

Li D, Tapscoft T, Gonzalez O Burch PE, Quinones MA, Zoghbi WA, Hill R, Bachinski LL, Douglas LM, Roberts R (1999)
Desmin mutation responsible for idiopathic dilated cardiomyopathy.
Circulation 100: 461-464.

Li H, Linke WA, Oberhauser AF, Carrion-Vazquez M, Kerkvliet JG, Lu H, Marszalek PE and Fernandez JM (2002)
Reverse engineering of the giant muscle protein titin.
Nature 418: 998-1002.

Lindstedt SL, Reich TE, Keim P and LaStayo PC (2002)
Do muscles function as adaptable locomotor springs?
J Exp Biol. 205: 2211-2216.

Linke WA, Popov VI and Pollack GH (1994)
Passive and active tension in single cardiac myofibrils.
Biophys J. 67: 782-792.

Linke WA, Ivemeyer M, Olivieri N, Kolmerer B, Rüegg JC and Labeit S (1996)
Towards a molecular understanding of the elasticity of titin.
J Mol Biol. 261: 62-71.

Linke WA, Ivemeyer M, Mundel P, Stockmeier MR and Kolmerer B (1998 a)
Nature of PEVK-titin elasticity in skeletal muscle.
Proc Natl Acad Sci USA 95: 8052-8057.

Linke WA, Stockmeier MR, Ivemeyer M, Hosser H and Mundel P (1998 b)
Characterizing titin's I-band Ig domain region as an entropic spring.
J Cell Sci. 111: 1567-1574.

Linke WA, Rudy DE, Centner T, Gautel M, Witt C, Labeit S and Gregorio CC (1999)
I-band titin in cardiac muscle is a three-element molecular spring and is critical for maintaining thin filament structure.
J Cell Biol. 146: 631-644.

Linke WA (2000)
Stretching molecular springs: Elasticity of titin filaments in vertebrate striated muscle.
Histol Histopathol. 15: 799-811.

Linke WA, Kulke M, Li H, Fujita-Becker S, Neagoe C, Manstein DJ, Gautel M and Fernandez JM (2002 a)
PEVK domain of titin: an entropic spring with actin-binding properties.
J Struct Biol. 137: 194-205.

Linke WA and Fernandez JM (2002 b)
Cardiac titin: Molecular basis of elasticity and cellular contribution to elastic and viscous stiffness components in myocardium.
J Muscle Res Cell Motil. 23: 461-464.

Linke, W.A. & J.M. Fernandez (2003)
Cardiac titin: Molecular basis of elasticity and cellular contribution to elastic and viscous stiffness components in myocardium, 483-497.
In: Linke, W.A, Granzier H, Kellermayer M (Hrsg): Mechanics of Elastic Biomolecules.
Kluwer: Dordrecht.

Liversage AD, Holmes D, Knight PJ, Tskhovrebova L, Trinick J (2001)
Titin and the sarcomere symmetry paradox.
J Mol Biol. 305: 401-409.

Makarenko I, Opitz CA, Leake MC, Neagoe C, Kulke M, Gwathmey JK , del Monte F, Hajjar RJ, Linke WA (2004)
Passive stiffness changes due to upregulation of compliant titin isoforms in human DCM hearts.
Circ.Res. 95: 708-716.

Marko JF and Siggia ED (1995)
Stretching DNA.
Macromolecules 28: 8759-8770.

Maruyama K, Matsubara S, Natori R, Nonomura Y, Kimura S, Ohashi K, Murakami F, Handa S and Eguchi G (1977 a)

Connectin, an elastic protein of muscle: characterization and function.

J Biochem. (Tokyo) 82: 317-337.

Maruyama K, Murakami F and Ohashi K (1977 b)

Connectin, an elastic protein of muscle. Comparative Biochemistry.

J Biochem. (Tokyo) 82: 339-345.

Maruyama K, Kimura S, Yoshidomi H, Sawada H and Kikuchi M (1984)

Molecular size and shape of β-connectin, an elastic protein of striated muscle.

J Biochem. (Tokyo) 95: 1423-1493.

McDonough JL, Arrell DK, Van Eyk JE (1999)

Troponin I degradation and covalent complex formation accompanies myocardial ischemia/reperfusion injury.

Circ Res. 84: 9-20.

Minajeva A, Kulke M, Fernandez JM and Linke WA (2001)

Unfolding of titin domains explains the viscoelastic behaviour of skeletal myofibrils.

Biophys J. 80: 1442-1451.

Minajeva A, Neagoe C, Kulke M and Linke WA (2002)

Titin-based contribution to shortening velocity of rabbit skeletal myofibrils.

J Physiol. 540: 177-188.

Morano I, Hadicke K, Grom S, Koch A, Schwinger RH, Bohm M, Bartel S, Erdmann E, Krause EG (1994)

Titin, myosin light chains and C-protein in the developing and failing human heart.

J Mol Cell Cardiol. 26: 361-368.

Moss RL and Fitzsimons DP (2002)

Frank-Starling relationship: long on importance, short on mechanism.

Circ Res. 90: 11-13.

Muhle-Goll C, Habeck M, Cazorla O, Nilges M, Labeit S and Granzier H (2001)

Structural and functional studies of titin's fn3 modules reveal conserved surface patterns and binding to myosin S1- a possible role in the Frank-Starling mechanism of the heart.]

J Mol Biol. 313: 431-447.

Nagueh SF, Shah G, Wu Y, Torre-Amione G, King NM, Lahmers S, Witt CC, Becker K, Labeit S, Granzier HL. (2004)

Altered titin expression, myocardial stiffness, and left ventricular function in patients with dilated cardiomyopathy.
Circulation 110: 155-162.

Nave R, Fürst DO and Weber K (1989)
Visualization of the polarity of isolated titin molecules: a single globular head on a long thin rod as the M Band anchoring domain?
J Cell Biol. 109: 2177-2187.

Neagoe C, Kulke M, del Monte F, Gwathmey JK, de Tombe PP, Hajjar R and Linke WA (2002)
Titin isoform switch in ischemic human heart disease.
Circulation 106: 1333-1341.

Neagoe C, Opitz CA, Makarenko I, Linke WA (2003)
Gigantic variety: expression patterns of titin isoforms in striated muscles and consequences for myofibrillar passive stiffness.
J Muscle Res Cell Motil. 24: 175-189.

Neuhoff V, Stamm R, Pardowitz I, Arold N, Ehrhardt W and Taube D (1990)
Essential problems in quantification of proteins following colloidal staining with coomassie brilliant blue dyes in polyacrylamide gels, and their solution.
Electrophoresis 11: 101-117.

Noble MIM (1977)
The diastolic viscous properties of cat papillary muscle.
Circ Res. 40: 288–292.

Obermann WM, Plessmann U, Weber K, Fürst DO (1995)
Purification and biochemical characterization of myomesin, a myosin-binding and titin-binding protein, from bovine skeletal muscle.
Eur J Biochem. 233: 110-115.

Obermann WM, Gautel M, Steiner F, van der Ven PF, Weber K, Fürst DO (1996)
The structure of the sarcomeric M band: localization of defined domains of myomesin, M-protein, and the 250-kD carboxy-terminal region of titin by immunoelectron microscopy.
J Cell Biol. 134: 1441-1453

Obermann WM, Gautel M, Weber K, Fürst DO (1997)
Molecular structure of the sarcomeric M band: mapping of titin and myosin binding domains in myomesin and the identification of a potential regulatory phosphorylation

site in myomesin.
EMBO J. 16: 211-220.

Opitz CA, Kulke M, Leake MC, Neagoe C, Hinssen H, Hajjar R J, Linke WA. (2003)
Damped elastic recoil of the titin spring in myofibrils of human myocardium.
Proc Natl Acad Sci USA. 100: 12688–12693.

Opitz CA, Leake MC, Makarenko I, Benes V, Linke WA. (2004)
Developmentally regulated switching of titin size alters myofibrillar stiffness in the perinatal heart.
Circ Res. 94: 967-975.

Ohtsuka H, Yajima H, Maruyama K, Kimura S. (1997)
Binding of the N-terminal 63 kDa portion of connectin/titin to alpha-actinin as revealed by the yeast two-hybrid system.
FEBS Lett. 401: 65-67.

Pfuhl M and Pastore A. (1995)
Tertiary structure of an immunoglobulin-like domain from the giant muscle protein titin: a new member of the I set.
Structure 3: 391-401.

Politou AS, Thomas DJ and Pastore A (1995)
The folding and stability of titin immunoglobulin-like modules, with implications for the mechanism of elasticity.
Biophys J. 69: 2601-2610.

Prado LG, Makarenko I, Andresen C, Krüger M, Opitz CA and Linke WA (2005)
Isoform diversity of giant proteins in relation to passive and active contractile properties of rabbit skeletal muscles.
J Gen Physiol. 126: 461-480.

Rief M, Gautel M, Oesterhelt F, Fernandez JM and Gaub HE (1997)
Reversible unfolding of individual titin immunoglobulin domains by AFM.
Science 276: 1109-1112.

Roy CS (1881)
The elastic properties of the arterial wall.
J Physiol. 3: 125–159.

Schaub MC, Hefti MA, Harder BA, Eppenberger HM.(1997)
Various hypertrophic stimuli induce distinct phenotypes in cardiomyocytes.
J Mol Med. 75: 901-920.

Scott K A, Steward A, Fowler SB, and Clarke J (2002)

Titin; a multidomain protein that behaves as the sum of its parts.

J Mol Biol 315: 819-829.

Tatsumi R and Hattori A (1995)

Detection of giant myofibrillar proteins connectin and nebulin by electrophoresis in 2% polyacrylamide slab gels strengthened with agarose.

Anal Biochem. 224: 28-31.

Trinick J, Knight P and Whiting A (1984) Purification and properties of native titin. *J Mol Biol.* 180: 331-356.

Trinick J and Tskhovrebova L (1999)

Titin: a molecular control freak.

Trends Cell Biol. 9: 377-380.

Trombitas K, Wu Y, Labeit D, Labeit S and Granzier H (2001)

Cardiac titin isoforms are coexpressed in the half-sarcomere and extend independently.

Am J Physiol Heart Circ Physiol. 281: H1793-H1799.

Trombitas K, Wu Y, McNabb M, Greaser M, Kellermayer MS, Labeit S, Granzier H. (2003)

Molecular basis of passive stress relaxation in human soleus fibers: assessment of the role of immunoglobulin-like domain unfolding.

Biophys J. 85: 3142-3153.

Tskhovrebova L, Trinick J, Sleep JA and Simmons RM (1997)

Elasticity and unfolding of single molecules of the giant muscle protein titin.

Nature 387: 308-312.

Tskhovrebova L, Trinick J (2000)

Extensibility in the titin molecule and its relation to muscle elasticity.

Adv Exp Med Biol. 481: 163-173.

Tskhovrebova L, Trinick J. (2002)

Role of titin in vertebrate striated muscle.

Phil. Trans. R. Soc. Lond. B 357: 199–206.

van der Ven PF, Furst DO (1997)

Assembly of titin, myomesin and M-protein into the sarcomeric M band in differentiating human skeletal muscle cells in vitro.

Cell Struct Funct. 22: 163-171.

Vemuri R, Lankford EB, Poetter K, Hassanzadeh S, Takeda K, Yu ZX, Ferrans VJ and

Epstein ND (1999)

The stretch-activation response may be critical to the proper functioning of the mammalian heart.

Proc Natl Acad Sci USA 96: 1048-1053.

Yamasaki R, Berri M, Wu Y, Trombitas K, McNabb M, Kellermayer MS, Witt C, Labeit D, Labeit S, Greaser M, Granzier H (2001)

Titin-actin interaction in mouse myocardium: passive tension modulation and its regulation by calcium/S100A1.

Biophys J. 81: 2297-2313.

Young P, Ferguson C, Bañuelos S, Gautel M. (1998)

Molecular structure of the sarcomeric Z-disk: two types of titin interactions lead to an asymmetrical sorting of alpha-actinin.

EMBO J. 17:1614-1624

Wang K, McClure J and Tu A (1979)

Titin: major myofibrillar component of striated muscle.

Proc Natl Acad Sci USA 76: 3698-3702.

Wang K, Ramirez-Mitchell R and Palter D (1984)

Titin is an extraordinary long, flexible, and slender myofibrillar protein.

Proc Natl Acad Sci USA 81: 3685-3689.

Wang K. and Wright J. (1988)

Architecture of the sarcomere matrix of skeletal muscle: immunoelecron microscopic evidence that suggests a set of paralell inextensible nebulin filaments anchored at the Z-line.

J. Cell Biol. 107: 2199-2212.

Wang K, McCarter R, Wright J, Beverly J and Ramirez-Mitchell R (1991)

Regulation of skeletal muscle stiffness and elasticity by titin isoforms: A test of the segmental extension model of resting tension.

Proc Natl Acad Sci USA 88: 7101-7105.

Weber KT. (1997)

Extracellular matrix remodelling in heart failure: a role for de novo angiotensin II generation.

Circulation 96: 4065-4082.

Whiting A, Wardale J and Trinick J (1989)

Does titin regulate the length of muscle thick filaments?

J Mol Biol. 205: 263-268.

Witt C. C., Olivieri N., Centner T., Kolmerer B., Millevoi S., Morell J., Labeit D., Labeit S., Jockusch H., and Pastore A. (1998)

A survey of the primary structure and the interspecies conservation of I-band titin's elastic elements in vertebrates.

J Struct Biol. 122: 206-215.

Wu Y, Cazorla O, Labeit D, Labeit S and Granzier H. (2000)

Changes in titin and collagen underlie diastolic stiffness diversity of cardiac muscle.

J Mol Cell Cardiol. 32: 2151-2162.

Wu Y, Bell SP, Trombitas K, Witt CC, Labeit S, LeWinter MM and Granzier H (2002)

Changes in titin isoform expression in pacing-induced cardiac failure give rise to increased passive muscle stiffness.

Circulation 106: 1384-1389.

7. CURRICULUM VITAE

PERSONALIEN

Name, Vorname: Neagoe, Ciprian
Geburtsdatum: 9. Oktober 1973
Geburtsort: Câmpina, Rumänien
Familienstand: ledig
Staatsangehörigkeit: rumänisch
Vater: Neagoe, Ion
Mutter: Neagoe, Veronica

SCHULISCHER WERDEGANG

1980 - 1988	Grundschule: Şcoala nr.1, Poiana-Câmpina, Prahova, Rumänien
1988 - 1992	Gymnasium: Liceul Teoretic "N. Grigorescu", Câmpina, Prahova, Rumänien
Juni 1992	Abitur

UNIVERSITÄRER WERDEGANG

WS 1992	Beginn des Physik-Studiums an der Universität von Bukarest, Rumänien
SS 1997	Abschluss des Studiums
Juni 1997	Staatsexamen, Diplom-Physiker, Fakultät für Physik, Universität von Bukarest, Rumänien
WS 1997 / SS 1998	Studium der Biophysik an der Universität von Bukarest, Rumänien
Juni 1998	Dissertation, Master in Physik (Vertiefte Studien in Biophysik), Fakultät für Physik, Universität von Bukarest, Rumänien

PROMOTION

WS 1998 / bis SS 2000	Promotionsarbeiten zum Dr. Biologie am Institut für Zelluläre Biologie und Pathologie „N. Simionescu“, Bukarest, Rumänische Akademie, Rumänien
SS 2000	Beginn der Promotion zum Dr. sc. hum. an der Ruprecht-Karls-Universität Heidelberg, Deutschland, Institut für Physiologie und Pathophysiologie, Arbeitsgruppe Prof. Dr. Linke
SS 2003	Ende der Promotionsarbeiten an der Ruprecht-Karls-Universität Heidelberg

BERUFLICHER WERDEGANG

Juli 1997/ bis jetzt	Wissenschaftlicher Angestellter (Assistent, Doktorand) am Institut für Zelluläre Biologie und Pathologie „N. Simionescu“, Bukarest, Rumänische Akademie
Juli 2000/ bis	Wissenschaftlicher Angestellter (Doktorand) an der Ruprecht-Karls-Universität Heidelberg, Deutschland, Institut für Physiologie und Pathophysiologie, Arbeitsgruppe Prof. Dr. Linke
Juni 2003	Ende der Promotionsarbeiten an der Ruprecht-Karls-Universität Heidelberg
WS 2003/ 2004/ bis SS 2004	Assistenz-Professor in Physik, Fakultät für Biologie, Universität von Bukarest, Rumänien

8. OWN PUBLICATIONS

ORIGINAL ARTICLES IN PEER-REVIEWED JOURNALS:

1) Neagoe C, Gafencu A, Heltianu C. (1998)

Transfection of type I receptor for immunoglobulin G in bovine aortic endothelial cells.

Current Problems in Cellular and Molecular Biology. 3: 378-383.

2) Neagoe C, Kulke M, del Monte F, Gwathmey JK, de Tombe PP, Hajjar RJ, Linke WA. (2002)

Titin isoform switch in ischemic human heart disease.

Circulation.106: 1333-1341.

3) Neagoe C, Makarenko I, Opitz CA, Linke WA. (2003)

Gigantic variety: expression patterns of titin isoforms in striated muscles and consequences for myofibrillar passive stiffness.

J Muscle Res Cell Motil. 24:175–189.

4) Makarenko I, Opitz CA , Leake MC, Neagoe C, Kulke M, Gwathmey JK, del Monte F, . Hajjar RJ, Linke WA. (2004)

Passive Stiffness Changes Due To Upregulation of Compliant Titin Isoforms in Human Dilated Cardiomyopathy Hearts.

Circ Res. 95: 708–716.

5) Opitz CA, Kulke M, Leake MC, Neagoe C, Hinssen H, Hajjar R J, Linke WA. (2003)

Damped elastic recoil of the titin spring in myofibrils of human myocardium.

Proc. Natl. Acad. Sci. USA 100: 12688–12693.

6) Hunter RJ, Neagoe C, Jarvelainen HA, Martin CR, Lindros KO, Linke WA, Preedy VR. (2003)

Alcohol affects the skeletal muscle proteins, titin and nebulin in male and female rats.

J Nutr. 133: 1154-1157.

7) Minajeva A, Neagoe C, Kulke M, Linke WA. (2002)

Titin-based contribution to shortening velocity of rabbit skeletal myofibrils.

J Physiol. 540: 177-188.

8) Linke WA, Kulke M, Li H, Fujita-Becker S, Neagoe C, Manstein DJ, Gautel M, Fernandez JM. (2002)

PEVK domain of titin: an entropic spring with actin-binding properties.

J Struct Biol. 137: 194-205.

9) Anderson J, Joumaa V, Stevens L, Neagoe C, Li Z, Mounier Y, Linke WA, Goubel F. (2002)
Passive stiffness changes in soleus muscles from desmin knockout mice are not due to titin modifications.
Pflügers Arch. 444: 771-776.

10) Kulke M, Neagoe C, Kolmerer B, Minajeva A, Hinssen H, Bullard B, Linke WA. (2001)
Kettin, a major source of myofibrillar stiffness in Drosophila indirect flight muscle.
J Cell Biol. 154: 1045-57.

11) Kulke M, Fujita-Becker S, Rostkova E, Neagoe C, Labeit D, Manstein DJ, Gautel M, Linke WA. (2001)
Interaction between PEVK-titin and actin filaments: origin of a viscous force component in cardiac myofibrils.
Circ Res. 89: 874-881.

9. ACKNOWLEDGEMENTS

This work was made possible through the contribution of several persons and here is the place to express my gratitude.

Prof. Dr. rer. nat. Wolfgang A. Linke generously provided the tutorship for this dissertation and the supervision for the experiments on which it is based. In this context, I express my gratitude for his permanent interest in improving my understanding of muscle physiology. Based on his previous important original contributions to titin research our group was able to generate new models and ideas and publish a series of high-ranking scientific articles that are mentioned in this dissertation. I am also grateful to him for his careful, friendly support he provided to me, guiding me on how to accommodate and live in Heidelberg during the three years (2000 - 2003) of this doctoral work.

Dr. sc. hum. Michael Kulke, then a Ph.D student, made major contributions to the experimental part of this work on titin isoforms. His suggestions and advice on some topics, as well as the results that we obtained together are gratefully acknowledged. I thank him not only for the exceptional scientific work he did for the papers we published in this period, but also for the advices he gave me in various life situations I met in Heidelberg. I could say that he protected me to stay away from trouble. I should not forget to mention that he sometimes picked me up with his car from the University Parking Place Im Neuenheimer Feld, over the bridge, up to the other side of the Neckar. That was very kind from him. Thank you once more!

The excellent technical support of **Mr. Rudolf Dussel** was essential in the laboratory. Thank you very much! It was an honour for me to know him and to have his generous attention and advice during my stay in Heidelberg.

Dr. med. Ave Minajeva, Ph.D contributed a lot to my rapid integration in the laboratory team. She did show me several things one should know when one is new in a lab and she also explained to me some technical details of the experimental work with animal tissue.

Dr. med. Christiane A. Opitz was a graceful and energizing presence in the laboratory. Her outstanding work on titin recoil and on developmentally regulated titin isoform expression was a scientific delight for me, especially because this started from some of the observations I now report in this dissertation.

Dr. Mark Leake did the mathematical modeling to predict the isoform modulation

of titin passive tension, published in Makarenko et al. (2004), and had, out of the record, of course, some nice ideas on how to overcome the physics laws. I really appreciated his performance of setting up an atomic force microscope after few months of work in the laboratory.

It was really useful to get technical support from Mrs**. Anita Kühner** when doing immunofluorescence on tissue sections. She also had her own ways of making me think that the time spent in the laboratory is not lost time.

Dr. Irina Makarenko quickly learned in the summer of 2002 all the techniques necessary to see titin on gels even at a better resolution I managed to get in many cases. This was really a technical success. I did like talking to her between two experiments and I do admire her strength and her will, at least as I could see them in the laboratory work.

Diplomphysiker Mr. Uros Krzic, now a Ph.D student, wrote the software for some special protocols of the Muscle Research System apparatus and for some measurements we did for the Makarenko et al. (2004) paper. It was nice to know him and to work with him. It was also interesting discussing with his supervisors at that time, **Prof. Dr. Belinda Bullard** and **Prof. Dr. Kevin Leonard,** some of the experiments he did.

My gratitude is expressed to all the people I knew at the Institute of Physiology and Pathophysiology, University of Heidelberg. They all had their contributions to the success of this doctoral work.

Acknowledgements are made to the people who kindly invited me to visit their laboratories and do the experiments which are mentioned in this thesis: **Prof. Dr. Dietmar J. Manstein,** at that time from the Max-Planck-Institute for Medical Research in Heidelberg, Germany, **Prof. Dr. Hans M. Eppenberger** from the Institute of Cell Biology, ETH Hoenggerberg, Zürich, Switzerland and **Dr. Monika Eppenberger-Eberhardt** and **Dr. Daniel A. Dätwyler**, his collaborators.

The current thesis is based on results that were published in several papers where I am co-author. I acknowledge the work of all the persons that contributed to these studies even if I did not know them personally. I like to mention **Dr. Roger Hajjar** and his team at the Massachusetts General Hospital and Harvard Medical School, Cardiovascular Research Center, Charlestown, USA. They are all mentioned in my publication list.

I now have the opportunity to thank **Acad. Prof. Dr. Maya Simionescu** from the Institute of Cellular Biology and Pathology "N. Simionescu", Bucharest, Romania, and all my present and former colleagues from this institute, who provided me support at the beginning of my scientific career. Some of them strongly encouraged me to finish this work:

Prof. Dr. Constantina Heltianu, M.Sc. Ovidiu Popa, Dr. Loredan Ştefan Niculescu, Prof. Dr. Felicia Antohe, Dr. Adriana Georgescu, Dr. Anca Gafencu, and Dr. Manuela Călin.

For the privilege of being a scientist I thank all colleagues and supervisors I had in my scientific career so far, I acknowledge the excellent study environement at the University of Heidelberg, but mostly I thank once more **Prof. Dr. Wolfgang A. Linke** who introduced me to science as a living concept served by dedicated scientists.